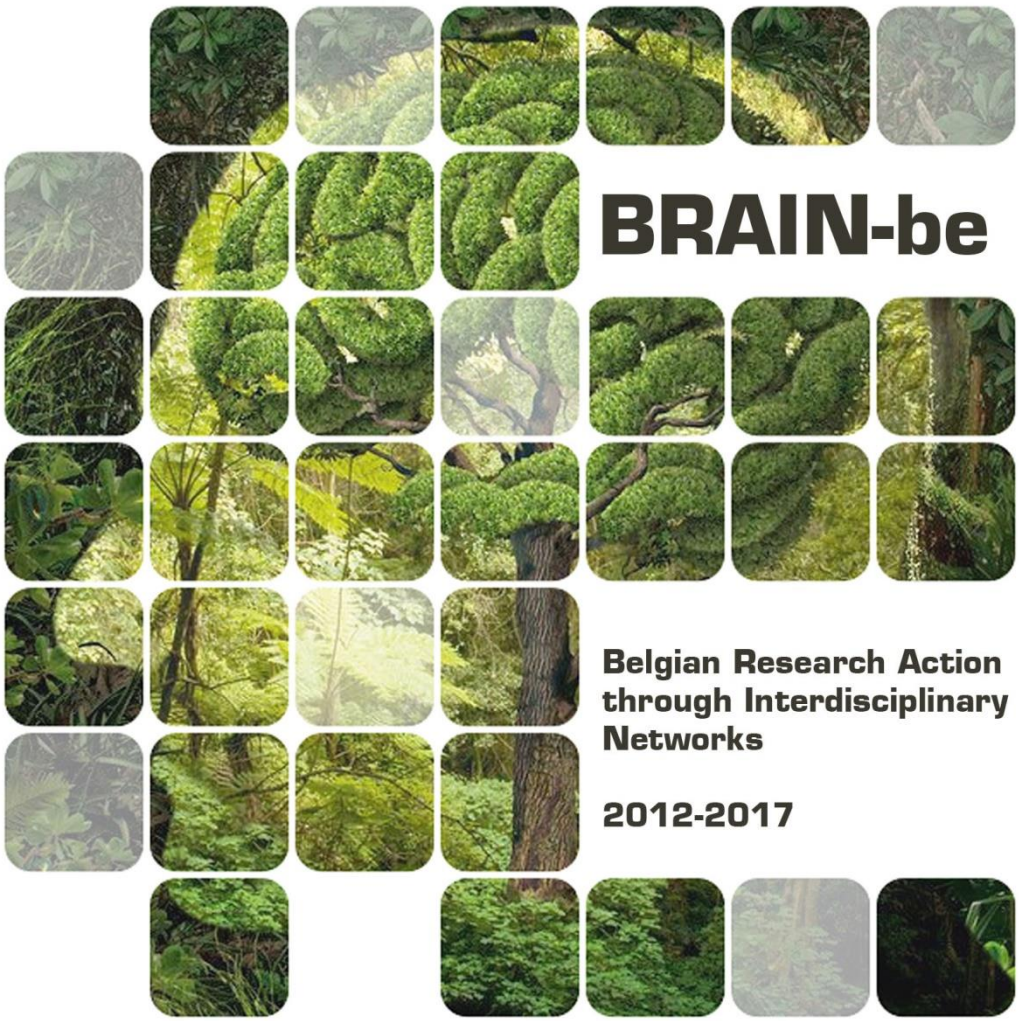

PERSUADE

Ex**PER**imental approaches towards Future **S**ustainable **U**se of North Sea **A**rtificial Har**D** Substrat**E**s

Jan Vanaverbeke (RBINS), Ulrike Braeckman (UGent), André Catrrijsse (VLIZ), Annabelle Dairain (UGent), Nele De Meester (UGent), Steven Degraer (RBINS) Tom Moens (UGent), Karline Soetaert (Royal NIOZ), Carl Van Colen, (UGent), Sven Van Haelst (VLIZ), Ellen Vlaminck (UGent), Helena Voet (RBINS)

Axis 1: Ecosystems, biodiversity and evolution

belspo .be

NETWORK PROJECT

PERSUADE

ExPERimental approaches towards Future Sustainable Use of North Sea Artificial HarD SubstratEs

Contract - BR/175/A1/PERSUADE - BR/175/A1/PERSUADE-2

FINAL REPORT

PROMOTORS: Jan Vanaverbeke / Steven Degraer (RBINS)
Tom Moens/Karline Soetaert/Carl Van Colen (UGent)
Jan Mees (VLIZ)

AUTHORS: Jan Vanaverbeke (RBINS), Ulrike Braeckman (UGent), André Catrrijsse (VLIZ), Annabelle Dairain (UGent), Nele De Meester (UGent), Steven Degraer (RBINS) Tom Moens (UGent), Karline Soetaert (UGent), Carl Van Colen, (UGent), Sven Van Haelst (VLIZ), Ellen Vlaminck (UGent), Helena Voet (RBINS)

museum NATURALSCIENCES.BE GHENT UNIVERSITY VLIZ belspo .be

Published in 2022 by the Belgian Science Policy Office
WTCIII
Simon Bolivarlaan 30 Boulevard Simon Bolivar
B-1000 Brussels
Belgium
Tel: +32 (0)2 238 34 11 - Fax: +32 (0)2 230 59 12
http://www.belspo.be
http://www.belspo.be/brain-be

Contact person: Koen Lefever
Tel: +32 (0)2 238 35 51

Jan Vanaverbeke (RBINS), Ulrike Braeckman (UGent), André Catrrijsse (VLIZ), Annabelle Dairain (UGent), Nele De Meester (UGent), Steven Degraer (RBINS) Tom Moens (UGent), Karline Soetaert (UGent), Carl Van Colen, (UGent), Sven Van Haelst (VLIZ), Ellen Vlaminck (UGent), Helena Voet (RBINS). ***ExPERimental approaches towards Future Sustainable Use of North Sea Artificial HarD SubstratEs***. Final Report. Brussels : Belgian Science Policy Office 2022 – 69 p. (BRAIN-be - (Belgian Research Action through Interdisciplinary Networks))

TABLE OF CONTENTS

ABSTRACT

PERSUADE investigated how climate change influences the known effects of fouling fauna in offshore wind farms on the marine environment and assessed how additional aquaculture activities within such OWF have added effects. We focused on three important fouling species (the blue mussel *M. edulis*, the amphipod *Jassa herdmani* and the plumose anemone *Metridium senile*) and two important sediment-inhabiting species (the sand mason *Lanice conchilega* and the white furrow shell *Abra alba*) to investigate how climate change (a combination of ocean warming and ocean acidification) would affect ecosystem functioning (focus on nutrient cycling and food webs) in OWF, and whether additional aquaculture activities would result in additional activities. In a second step, we developed new in-situ and experimental techniques and equipment allowing for community-wide experiments and subsequent modeling, paving the way towards a better understanding of the effects of multiple human activities in a changing environment. Our results indeed show that the presence of offshore wind farm has important consequences for the marine environment, ranging from the release of the potent greenhouse gass N_2O to filtering large amounts of sea water. Climate change generally altered these effects, both in the water column and the sediment, caused by behaviourial adaptations of organisms surviving in a warming and acidifying environment. Our modeling work suggests that climate change will not have an adverse effect on bivalve aquaculture within OWFs but suggest a competition for food with the fouling fauna on the turbines and indicate an increased release of N_2O in future climate conditions.

Keywords: offshore wind farms, bivalve aquaculture, climate change, food web, nutrient cycling, ecological modelling

1. INTRODUCTION

Recently, ocean sprawl – the proliferation of artificial structures in the sea (Duarte et al. 2013) – is moving further offshore, not in the least due to the increasing construction of offshore wind farms (OWF) in an attempt to the energy revenue from renewable sources. In 2020, 6651 turbines were operational in 112 offshore wind farms in Europe, which is predicted to increase to 16850 turbines in 172 offshore wind farms in 2030 (Soares-Ramos et al. 2020). They provide subtidal artificial hard substrate in areas dominated by soft sediments, and they span the entire water column, creating intertidal habitat in offshore areas. Both the turbines and the surrounding scour protection layers are inhabited by large numbers of colonizing fauna (Degraer et al. 2020), arranged along a vertical gradient (De Mesel et al. 2015) and attracting larger crustaceans (Krone et al. 2013) and benthic and benthopelagic fish (Reubens et al. 2014, Mavraki et al. 2020a). This fauna affects primary producer stocks in the water column (Slavik et al. 2019, Mavraki et al. 2020c), the spatial distribution of organic matter deposition (Ivanov et al. 2021), benthic mineralization processes (De Borger et al. 2021) and spatial distribution of macrobenthos (Coates et al. 2014).

While it is clear that the presence of OWF results in both local and regional changes, these changes need to be investigated in the context of global change. Sea surface temperatures in European waters are increasing at a rate of 0.2 °C per decade (EEA 2022) and pH is decreasing as the oceans absorb 25% of the annual anthropogenic CO_2 emissions i.e., 26.8 Gton CO_2 between 1994 and 2007 (Watson et al. 2020). The combination of warming and acidification leads to modifications of animal behaviour which ultimately cascade into altered species interactions and ecological processes (Nagelkerken & Munday 2016). As such, it is to be expected that functional changes observed because of the presence of OWF will interact with change caused by OWF.

On top of an increasing installation of OWF, the marine coastal area is increasingly being used for aquaculture activities. In response to this emerging Blue Growth activity but anticipating on the race for space in the marine area, the Belgian Marine Spatial plan allows for colocation of OWF installations with aquaculture installations. Judging from recently finished (EDULIS) or ongoing (H2020 UNITED) projects, the development of bivalve (blue mussel *Mytilus edulis*) or flat oyster (*Ostrea edulis*) aquaculture in Belgian OWF zones seems realistic. While structurally, this encompasses an increase in densities and biomass of a species of commercial interest, it can have far reaching functional consequences. Bivalves are suspension feeders, filtering large quantities of organic matter from the water column (Kellogg et al. 2013); they provide surface for biofilms involved in nutrient cycling (Stief 2013) and deposit faecal pellets to the sediment beneath the installations (Gadeken et al. 2021), thereby affecting both the water column and the local benthic-pelagic coupling. While aquaculture in the current conditions is an efficient way to harvest proteins from the marine environment (van der Schatte et al. 2020), the future of this activity is uncertain as the ocean acidification aspect of climate change hampers the development of bivalve early life stages (Tan & Zheng 2020).

It is clear that the combination effects of local human activities – including multi-use of the marine space – and global change (ocean warming and ocean acidification) will lead to changes in the marine environment. However, as such changes might be non-linear (synergistic or antagonistic), they are difficult to predict without targeted research based on experimental approaches and

careful upscaling to the real environment. Such approach would lead to an increased understanding of the functioning of marine ecosystems in future climate settings and guide local policy makers in decision-making processes concerning the sustainable use of the marine space.

2. STATE OF THE ART AND OBJECTIVES

Future coastal ecosystems will be challenged with a multitude of ecosystem-level stressors, resulting from both *local* anthropogenic activities and environmental change acting at the *global* scale. The installation of offshore wind farms (OWFs) is currently a major human activity in the coastal North Sea area, resulting in the introduction of large surfaces of artificial hard substrates (AHSs) in an otherwise sandy environment. These AHS are rapidly colonized by large quantities of fouling fauna, including non-indigenous species (NIS) (De Mesel et al. 2015). This in turn attracts fish (Reubens et al. 2014, Mavraki et al. 2021) and large crustaceans (Krone et al. 2017), and affects local phytoplankton communities (Slavik et al. 2019, Mavraki et al. 2020c) and organic matter deposition (Ivanov et al. 2021), cascading in altered sediment properties, sediment-inhabiting fauna (Coates et al. 2014, Hutchison et al. 2020) and carbon mineralisation pathways (De Borger et al. 2021).

Currently, most OWF are installed in coastal ecosystems, which are well-known sites of N-removal through microbial activity, thereby counteracting eutrophication processes (Seitzinger 2000). A drawback of this process is the production of N_2O during the first step of nitrification or by 'nitrifier denitrification' (see Heisterkamp et al. 2013). N_2O is a highly potent greenhouse gas that significantly contributes to global warming (Forster et al. 2007) and the destruction of the stratospheric ozone layer (Ravishankara et al. 2009). While the effect of macrobiota on N-cycling is mainly investigated in sediments (i.e. Braeckman et al. 2014), there is recent evidence that fouling fauna can contribute substantially to N_2O production, either through their own activity or through their microbiome (Heisterkamp et al. 2013, Moulton et al. 2016). As such, the presence of large quantities of fouling fauna on OWF can have important consequences for the air-sea exchange of greenhouse gasses in coastal areas, and therefore have a negative feedback on climate regulation, which is then strengthened by adding large quantities of bivalves through aquaculture activities.

Finally, all of these local effects need to be evaluated in the light of climate change, as a lot of the currently quantified effects of the presence of OWF and/or bivalve aquaculture operations are susceptible to climate change and therefore the capacity of the marine ecosystem to remove nutrients or provide food (Kitidis et al. 2011, Braeckman et al. 2014b, Tan & Zheng 2020, Liberti et al. 2022).

The general objective of PERSUADE was therefore to investigate **ecosystem-wide responses** to local and global stressors to quantify how future anthropogenic activities will contribute to the **production of the greenhouse gas** N_2O in a **future climate setting**, by quantifying the interactions between the **biotic and abiotic compartments in an OWF environment**. At the same time, we will investigate how **the transfer of energy** among the **different compartments of the coastal ecosystem** will evolve. By integrating the results in an **ecosystem model**, we will be able to run **climate impact scenarios** at scales (temporal, ecosystem-wide, with and without aquaculture) that are relevant for the sustainable **management** of the coastal ecosystem.

3. METHODOLOGY

PERSUADE research focused on investigating behavioral responses of key fouling and benthic species in current and future climate settings and on quantifying resulting changes in ecosystem processes. Key fouling species included the blue mussel *Mytilus edulis* (dominant in the infralittoral zone of the turbines), the tube-building amphipod *Jassa herdmani* (dominant in the sublittoral zone of the turbine) and the plumose anemone *Metridium senile* (dominant at the lower part of the turbine) (Fig. 1).

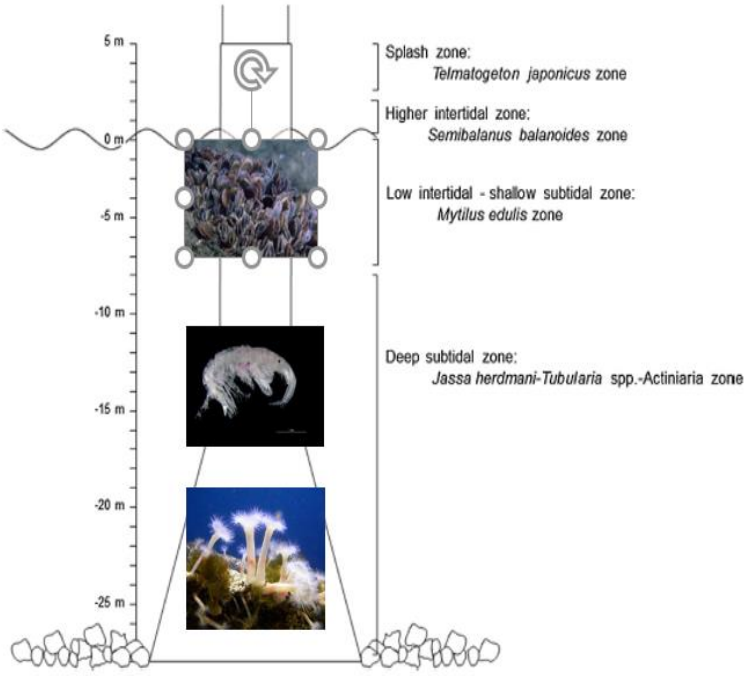

Figure 1. Fouling fauna key species, with indication of the depth zone on a turbine where they are dominant (modified from De Mesel et al. 2015)

The relative importance of these model species in the overall OWF ecosystem, i.a. in terms of total densities, filtration capacity and competitional dominance (Jak & Glorius 2017, Coolen et al. 2020), makes them ideally suited to assess functional implications at OWF AHS community level. Given the importance of the microbiome inhabiting outer bivalve shells (Heisterkamp et al. 2013) for N_2O production, we used additional molecular techniques to document the effect of climate change on the structural and functional composition of the biofilm.

In the sediment, key species in the Belgian part of the North Sea are the white furrow shell *Abra alba* and the sand mason *Lanice conchilega* (Braeckman et al. 2010) (Fig. 2). Especially *L. conchilega* is observed in increasingly higher abundances in sediments adjacent to the OWF turbines (Lefaible et al. in prep., Braeckman et al. 2020). The biodiffusion and sediment ventilation activity of *A. alba* and *L. conchilega*, respectively, stimulate sediment biogeochemistry (Braeckman et al. 2010).

Figure 2: The white furrow shell Abra alba *(left) and the sand mason* Lanice conchilega *(right). Pictures by Ulrike Braeckman and Hans Hillewaert.*

As the PERSUADE research strategy involved experimental work with benthos and fouling fauna, experimental methodology to conduct species specific, community- and ecosystem-wide experiments needed to be developed. While sampling of sediment-inhabiting organisms for incubation in experimental set-ups is standard practice, this was not at all the case for fouling organisms. These are generally collected by scraping them from a hard substrate (De Mesel et al. 2015, Mavraki et al. 2020a), thereby often damaging the organisms and making them unsuitable for further experimental work. Therefore, the methodological strategy for PERSUADE consisted of developing (1) an Artificial Hard Substrate Garden to harvest undamaged fouling organisms for further experimental work; (2) an experimental setting for climate change experiments on the individual species; (3) large-scale experimental systems allowing climate change-related functional research at the ecosystem scale, and (4) ecological models to upscale the experimental results to the level of the OWF.

3.1 Artificial Hard Substrate Garden

The design of the Artificial Hard Substrate Garden (AHSG) needed to comply with several boundary conditions.

1. Hard substrates were to be provided on a mooring where divers could sample the epifauna and bring it to the surface without scraping the organisms off the substrate. The AHSG needed to provide the opportunity to collect the entire community without damaging the biolayer.
2. The substrates needed to be sampled by divers, because bringing an entire mooring on deck of a vessel causes significant loss of fauna.
3. A standard sampling of the epifauna was a prerequisite and each sample was provided by a plastic plate of 150x150mm. Each mooring had to provide enough samples (approx. 50 / mooring).
4. An easy and fast collection of the substrates by divers.
5. A lightweight compact mooring that can be quickly located by the dive team.
6. The AHSG needed to provide fauna from the surface waters, from midwater and from near the seabed.

The environmental conditions created extra issues for the design. Tidal currents in the area where the AHSG needed to be moored can mount above 1.5Kn. Attempting to minimize the impact of

currents on the mooring, the structure holding the artificial substrates was kept to a minimum size and consequently a 3D shape was needed. A spherical shape would have better hydrodynamic characteristics to withstand tidal currents, but a box shape was finally choosen as its construction is much easier and cheaper. Using a box shape also allowed all substrates to be positioned in a similar direction in the water column.

Each cage measures 800x800x800mm and is made of galvanized L-profiles with lats on the side for further reinforcement and for mounting the artificial substrate plates. Each side of the cube can hold 12 plates. The top and bottom sides of the cube can also hold the same number of plates if needed (Fig. 3).

Figure 3. Cage of the AHSG mooring, holding 48 plates

The cages were anchored with a concrete block and the cage was maintained at the desired depth with a subsurface and a surface float. As the project continued, the mooring underwent several technical changes and adaptations to remediate problems encountered:

- The first trial included a rope between the cage and the anchor weight and between the cage and the surface float. The cage was attached with 4 short chains to the rope.
- The ropes were too susceptible to biofouling which increased their weight and caused sinking of the cage. A second setup used only chains to connect the anchor, cages and floats
- To minimize the impact of waves, smaller surface floats were used in a second trial and extra subsurface floats were used.
- The weight of the anchor was increased.

In the final design, the cages were attached to an anchor weight of 1250 kg. The mooring chain was kept to 10mm diameter. From the bottom and top side of the cage a chain sling (4legs) attached the cage to the mooring chain line. The cube, chainslings and the plates weigh approx. 50kg.

Surface floats were omitted in the final design as the wave impact caused loss of the surface floats and that also exerted too much force on the total mooring. Surface floats help divers to locate the mooring immediately and were initially provided for that purpose. In case a dive team needs too much time to locate the mooring, they may lack time for a complete sampling. An experienced dive team can relocate a mooring relatively fast without the surface floats if the position of the mooring is well registered when deployed.

The top of each mooring line held a 250L subsurface float to keep the mooring at the desired depth. The surface cage, which is moored at 5m depth, caused a navigational hazard and needed a surface marking buoy. This surface buoy was eventually omitted, and the cage was positioned at 7m depth as a compromise, significantly reducing any risks for navigation in the area.

All substrate plates were mounted to the frame with plastic tie wraps that could easily be cut by divers. To prevent loss of plastic tie wraps while collecting the plates, each tie wrap holding the plate to the frame was fixed to the plate with another tie wrap. After cutting the tie wrap, the plate was placed in a plastic bag and sealed before bringing it to the surface.

The design of the mooring allowed to keep the cage in place for over one year. Moorings were placed in early spring and recovered before winter. After a full spring and summer, the cages and floats can become overgrown with epifauna to such an extent that the total weight effectively diminishes or even exceeds the floating capacity of the subsurface float. Upon retrieval, components that got corroded or degraded were replaced for the redeployment.

3.2. Climate change experiments : single-species experiments and molecular approach

3.2.1 General set up

PERSUADE research was directed towards investigating the separate and combined effects of climate change (respectively ocean warming (OW), ocean acidification (OA) and the integrated Climate Change (CC)) on individual fouling fauna or sediment inhabiting key species. Therefore, a generic experimental system, allowing controlled manipulation of temperature and pH to which dedicated experimental units for fouling of benthic fauna were connected, was set up.

The general system consists of a series of header tanks (2000 – 4000 liter), where the water remained unmanipulated (control treatment – CTRL), or where temperature, pH or both were manipulated. Seawater temperature was regulated using TECO TK2000 heaters or Aqua Medic Titan 8000 professional units. pH was manipulated by controlled bubbling of seawater with 100% CO_2 using an IKS AquaStar aquaristic computer system or a personalized Fleuren & Nooijen JUMO microprocessor. Glass pH electrodes were calibrated weekly using Hanna Instruments ™ NIST Buffer Solutions (4.01 and 7.01). All temperature and pH data were logged every 15 minutes throughout the experiments with the IKS Aquastar system. Tank water was further sampled weekly and filtered through GF/C filters for determination of Total Alkalinity (TA) using a CONTROS HydroFIA™TA alkalinity system. The carbonate chemistry of the seawater was calculated using the CO_2SYS software (Pierrot et al. 2006) and thermodynamic constants (Mehrbach et al. 1973).

3.2.2 Fouling fauna experiments: ecophysiology

*Experimental set-up (*after (Voet et al. 2022)

Ecophysiological responses of the key fouling species to changes in ocean warming, ocean acidification and the integrated climate change effect were investigated during a 6-week experiment (Fig. 4) to arrive at a newly developed community-wide metric, the so-called maximized cumulative clearance potential. In summer 2017, 2018 and 2019, hard-substrate fauna was collected from turbine D6 in the C-Power wind farm (51°33.04'N - 02°55.42'E), as well as from an aquaculture pilot project approximately 10km off the Belgian coast (51°11.02'N - 02°39.88'E). *Mytilus edulis* was sampled by hauling an aquaculture longline on deck, while *Jassa herdmani* and *Metridium senile* were collected from the OWF turbine foundation by scientific divers at 7m and 18m depth, respectively. All samples were stored in aerated seawater and transported to the experimental facilities within 4 hours. All animals were randomly assigned to one of four experimental treatments. *Mytilus* individuals (n_{TOT} = 800) with an average length of 44.76 ± 0.42mm (SE) were distributed across four identical aquaria (100 x 45 x 70cm) equipped with a continuous flow-through mechanism with a total of approximately 400L in circulation per system, allowing for homogenisation of the seawater. *Jassa* individuals (n_{TOT} = 600; length > 5mm) were equally divided among a total of 12 cylindrical aquaria (Ø 12cm x h 25cm) equipped with a 1mm mesh for the animals to attach to (Mavraki N., personal communication, 2018). *Metridium* individuals (n_{TOT} = 480) with an average pedal disc diameter of 24.13 ± 0.53mm (SE) were divided among 12 replicate aquaria (40 x 20 x 30cm). All experimental units were connected to the experimental system as described in section 3.2.1.

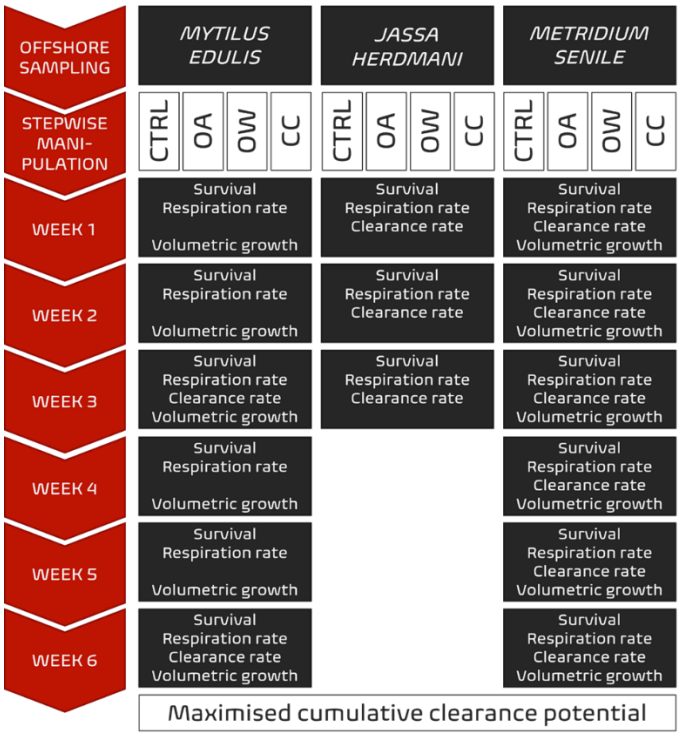

Figure 4 Methodology flowchart (CTRL: control, OA: ocean acidification, OW: ocean warming and CC: climate change).

After allowing the animals to acclimatise for 48h under ambient conditions, seawater temperature was increased by 1°C per day and pH was decreased by 0.1 pH unit per day for three days, resulting in seawater of +3°C and/or -0.3 pH units in the corresponding treatments compared to the control settings. The level of manipulation was chosen in accordance with the IPCC RCP8.5 projections for ocean warming and acidification towards the end of this century. These conditions were maintained for 21 days in the *Jassa* experiment and 42 days in the *Mytilus* and *Metridium* experiments.

Survival in each experimental treatment was monitored every two to three days throughout the experiment using a dedicated batch of individually numbered organisms (*M. edulis* and *M. senile*) or using the total population in the aquaria (*J. herdmani*). Dead animals were routinely removed from the aquaria. The overall high mortality of *Jassa* individuals limited the duration of this experiment to three weeks, as opposed to the six-week *Mytilus* and *Metridium* experiments. The ecophysiological parameters measured for all three species were respiration rate (RR) and clearance rate (CR).

Volumetric growth was measured for *M. edulis* and *M. senile* (*J. herdmani* was excluded because it moults). To measure RR and CR, triplicated individual closed-core incubations were set up in each experimental treatment. Each incubation core held one individual, along with manipulated seawater from the respective treatment, and was kept at the correct temperature throughout the incubations. Seawater inside was kept in motion to ensure an evenly mixed water column using either stirring discs (Fig. 5). (*M. edulis* and *M. senile*) or a shaking table (*J. herdmani*). The incubation core volume was corrected with the biovolume (mL) of *Mytilus* and *Metridium* individuals, measured by water displacement in a 500 ± 2mL graduated cylinder, while the biovolume of *Jassa* individuals was considered negligible.

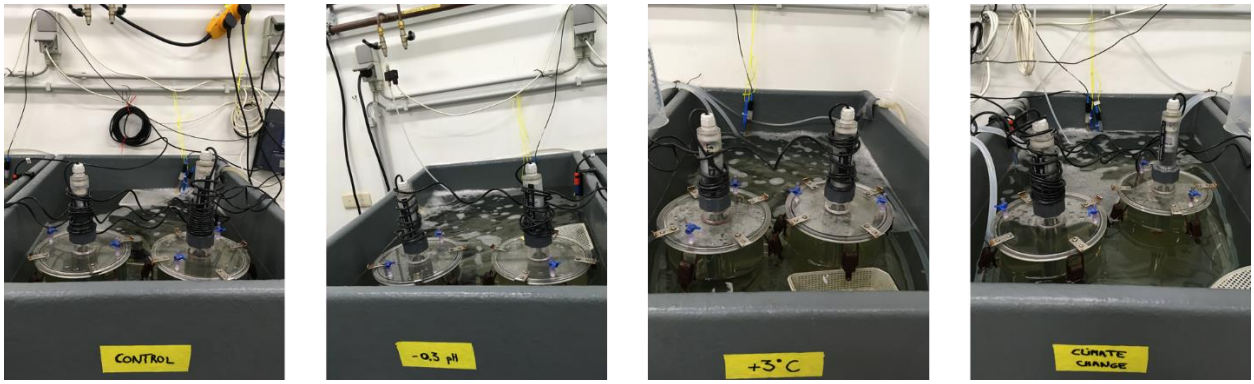

Figure 5 Experiment set-up

Survival (%) was calculated as the proportional survival per experimental treatment, with 100% survival at the start (day 0), according to Equation 1:

Equation 1 $$\text{Survival (\%)} = \frac{N_i}{N_0} \times 100$$

with N_0 and N_i the number of living individuals in the dedicated batch of organisms in each experimental treatment at day 0 and day i of the experiment, respectively. The number of individuals in each experimental treatment dedicated to the monitoring of survival was $N_0 = 75$ for *M. edulis*, $N_0 = 132$ for *J. herdmani* and $N_0 = 58$ for *M. senile*.

Respiration rates (RR) were assessed from the decrease in dissolved oxygen during the closed-core incubations. Seawater oxygen concentration (µmol L^{-1}) inside the incubation cores was measured continuously (*M. senile* and *J. herdmani*) or discretely (*M. edulis*) using PyroScience™ robust optical oxygen probes (*M. edulis* and *M. senile*) or sensor spots (*J. herdmani*) with REDFLASH-technology connected to a PyroScience™ FireSting O_2 logger. The closed-core respiration measurements were done weekly in a volume of 1.5L, 8.15L or 5mL and lasted 3h, 2.5h or 1h for *M. edulis*, *M. senile* and *J. herdmani*, respectively. Respiration rates were calculated using Equation 2 (*M. edulis*) or Equation 3 (*J. herdmani* and *M. senile*):

Equation 2 $$RR\ (\mu mol\ g^{-1}\ h^{-1}) = \frac{V\ (C_0-C_1)}{g\ (t_1-t_0)}$$

Equation 3 $$RR\ (\mu mol\ g^{-1}\ h^{-1}) = \frac{V}{g} \times \text{regression slope}$$

where V is the seawater volume (L) of the incubation core after correction for the biovolume of the organism, C_0 and C_1 are the respective dissolved oxygen concentrations (µmol L^{-1}) at the start and end t_0 and t_1 (h) of measurement, respectively, g is the dry weight (g) of the animal's soft tissue, and the regression slope is that of the linear regression through continuous oxygen measurements. A separate, simultaneous incubation for each experimental treatment was used to correct for background changes in dissolved oxygen, e.g. due to bacterial respiration or phytoplankton photosynthesis.

Clearance rates (CR), as a measure of the volume of water cleared by the organism, were calculated as the decline in algal cells, *Artemia* nauplii or mixed zooplankton over time in the incubation cores with *M. edulis*, *J. herdmani* and *M. senile*, respectively. To do this, incubation cores with and without organisms were set up in each experimental treatment and a known quantity of the respective food items was added to each core. The CR incubations were done in week 3 and 6 of the *M. edulis* experiment and weekly in the *J. herdmani* and *M. senile* experiments. After an initial mixing period of 30 minutes, discrete water samples were taken every 50 minutes throughout the 150-minute incubation with *M. edulis* and every 30 minutes throughout the 90-minute incubation with *J. herdmani* and *M. senile*.

Algal cell concentrations were determined using a BECKMAN Coulter Multisizer (100μm aperture) and the number of *Artemia* nauplii or assorted zooplankton was determined using a HydroptiC zooSCAN. Clearance rates were calculated according to Equation 4, following Riisgård (2001) and Coughlan (1969):

Equation 4 $$R\ (L\ g^{-1}\ h^{-1}) = \frac{V}{g \times t}\left(\ln\frac{C_1}{C_0} - \ln\frac{C_1'}{C_0'}\right)$$

where V is the seawater volume of the incubation core (L), corrected for the biovolume of the organism; g is the dry weight (g) of the animal; t is the duration of the incubation (h); C_0 is the food concentration at the start of the incubation, C_1 is the concentration at the end, while C_0' and C_1' are the food concentrations at the start and end of the empty control incubation, respectively. For every calculation, the condition of linearity of

$\ln\frac{C_0}{C_1}$ i in Equation 4 was confirmed (Riisgård 2001).

Volumetric growth (%) was calculated using weekly measurements of individually numbered *Mytilus* (n_{tot} = 72) and *Metridium* (n_{tot} = 48) individuals in all four experimental treatments. *Mytilus* individuals were measured weekly in three dimensions (length x width x height) to calculate the volume of an ellipsoid, approximating the shape of the closed mussel shell (Equation 5; Figure 4). The volume of an ellipsoid can be described as:

Equation 5 $$V\left(cm^3\right) = \frac{4}{3}\pi \times a \times b \times c$$

with a, b and c (cm) the three axes of the ellipsoid and the double axes 2a, 2b and 2c (cm) the length, width and height of the closed mussel shell, respectively (Figure 6).

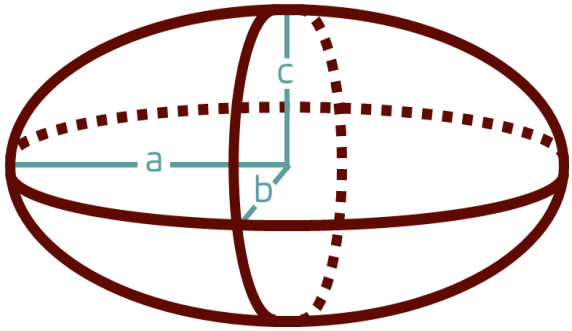

Figure 6. Ellipsoid (with three axes a, b and c) as an approximated volume of a closed mussel shell.

The growth of *Metridium* individuals was calculated by measuring the displaced water of the animal as a proxy for its biovolume (mL). Volumetric growth was expressed as percentage in- or decrease in ellipsoid volume (cm^3, *M. edulis*) and biovolume (mL, *M. senile*) compared to that at the start of the experiment (Week 0).

Maximised cumulative clearance potential was then calculated based on the ecophysiological results obtained in the experiment and published results (Voet et al. 2022). Using the mean individual biomass ($gDW\ ind^{-1}$), total density ($ind\ m^{-2}$) and total surface area (m^2) occupied by *M. edulis*, *J. herdmani* and *M. senile*, the estimated total biomass (gDW) present on a monopile foundation was calculated. These species-specific total biomasses were multiplied with the species-specific mean clearance rates ($L\ gDW^{-1}\ h^{-1}$) and corrected with the respective proportional survival (%) and the estimated fraction of feeding individuals (%), since thumbed *J. herdmani* males do not feed excessively (estimated to make up ± 16% of individuals in the field (Beermann & Franke 2012). These results were then amended according to the CTRL and CC treatments to estimate the species-specific total volume of seawater potentially cleared around a monopile foundation per day ($m^3\ d^{-1}$) in current and future climate (CTRL and CC, respectively) and subsequently summed, which was justified by this region's well-mixed water column (van Leeuwen et al. 2015). Monopile foundation dimensions were used to convert these calculated total volumes into a more perceivable measure, the *maximised cumulative clearance potential*: the estimated radial distance around the monopile foundation (m) equal to the width of a cylindrical sleeve with a volume equivalent to the seawater volume being cleared daily due to the presence of the AHS epifaunal community (Fig. 7).

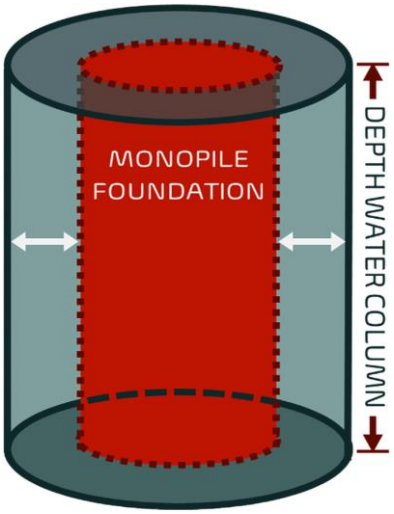

Figure 7. Schematic representation of the cumulative clearance potential as a cylindrical sleeve of seawater around a monopile foundation, with width = radial distance (white arrows) and height = depth of the water column (from Voet et al. 2022

Data Analysis (from Voet et al. 2022)

A Cox proportional hazards regression model was fitted for mortality events in each species. The effect of the manipulated experimental treatments on survival, compared to that in CTRL, was evaluated using hazard ratio (HR) with 95% confidence intervals. Additionally, a pairwise proportion test with Bonferroni correction was used to test for differences in survival between all four treatments at the end of the experiment.

The effects of temperature (current or elevated) and pH (current or lowered) on the ecophysiological parameters were investigated using a series of linear mixed effects models, where incubation core, individual organism identity and/or time (weekly incubations) were added as random factors to the models. If none of the random factors significantly contributed to explained left-over variance, a linear regression model was fitted. Significance of the two-way interaction 'temperature x pH' and post-hoc pairwise comparison of the group means were used to identify possible additive, synergistic, antagonistic or potentiating combination effects of increased temperature and lowered pH. For each parameter, normality of the residuals and model assumptions were checked, and data was transformed if necessary. Appropriate Gaussian or Gamma error distributions were used and model selection was based on the parametric bootstrap and Kenward Roger methods for mixed model comparison (Halekoh & Højsgaard 2014).

Analyses were conducted using R v3.6.1 with RStudio v1.4.1106 (RStudio Team 2016; R Core Team 2019). Cox survivorship models were fitted using the R packages *survival* (Therneau 2021) and *coxed* (Kropko & Harden 2020), linear regression models were fitted using the *stats* package (R Core Team 2019), linear mixed effects models were built using the R package lme4 (Bates et al. 2015) and the conditional R^2 (R^2c) for linear mixed effects models (to be interpreted as the variance explained by the entire model, including both fixed and random effects) was calculated using the *MuMIn* package (Barton 2020).

Species-specific mean clearance rates were summed to estimate the maximised cumulative clearance potential of the OWF AHS community and an appropriate cumulative standard error on this estimate was calculated by taking the square root of the quadratically summed standard deviations (i.e. the summed variances), considering the species-specific mean clearance rates are derived from independent experimental set-ups. The estimated cumulative clearance potential was compared between both current and future climate (CTRL and CC, respectively) using an ANOVA approach for summarised data in the R package *rpsychi* (Okumura 2012).

3.2.3. Fouling fauna experiments: N_2O production

In order to quantify N_2O emissions by bivalves, with emphasis on the contribution of the shell biofilm to the total N_2O production, and to improve understanding of the N_2O production pathway, a series of experiments were initiated using the general set-up as described above. N_2O can be the product of several processes within the nitrogen cycle. This was investigated by a combination of experiments in which some of the pathways were chemically blocked (all N_2O is then produced in the 'allowed' pathways) or through tracing sources of N_2O using a dual stable isotope approach (Fig. 8).

Experimental set-up (based on Voet et al. in prep.)

In summer 2018 and 2020, a respective total of 800 and 240 adult blue mussels (*Mytilus edulis*), with a mean soft tissue dry weight ± SD of 0.79 ± 0.28g, were sampled from a *M. edulis* longline in an offshore aquaculture pilot project approximately 10km off the Belgian coast (51°11.02'N - 02°39.88'E).

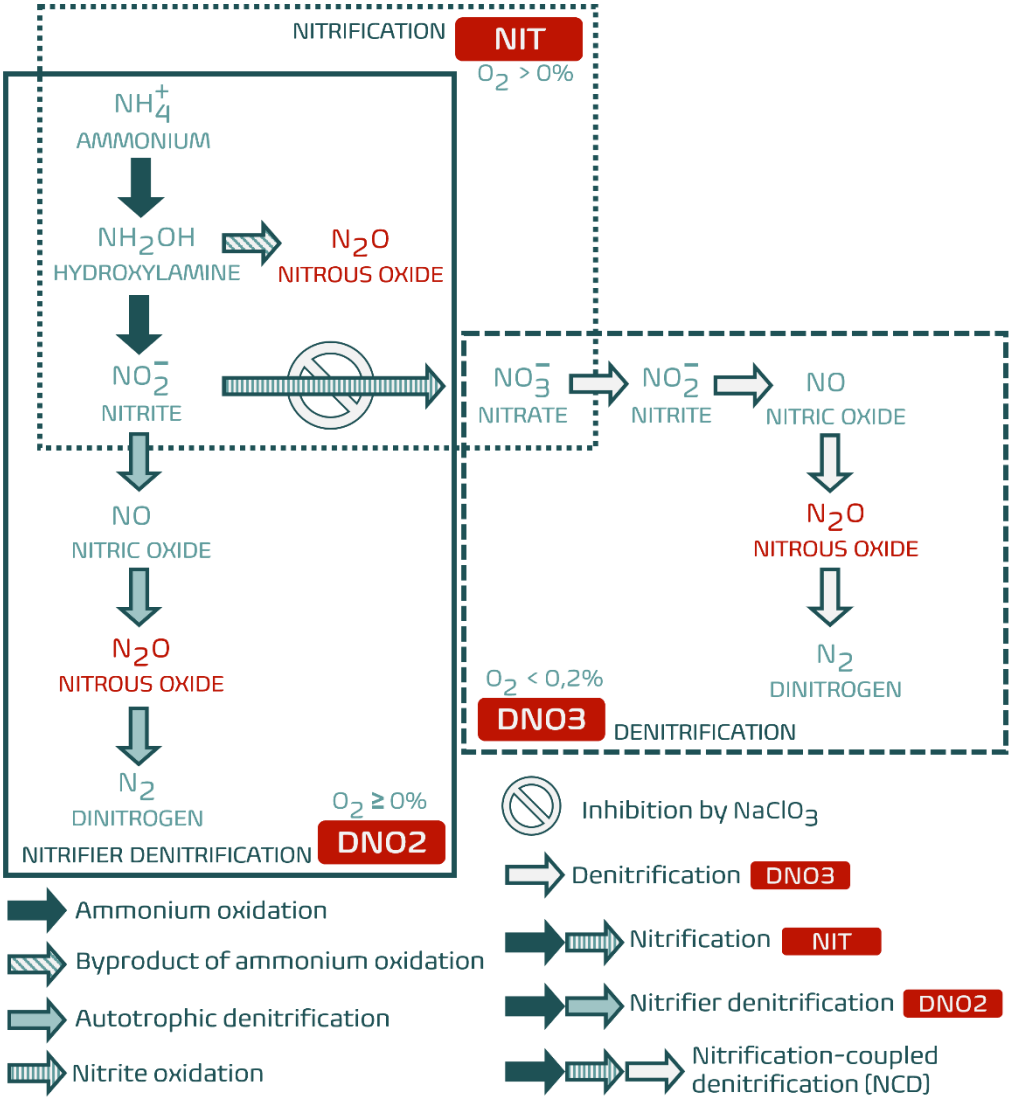

Figure 8. – Relevant pathways in the marine nitrogen cycle with possible sources of N_2O emission [NIT: oxic nitrification; DNO2: suboxic nitrifier denitrification; DNO3: anoxic denitrification in NCD] and targeted inhibition by $NaClO_3$. Adapted from Zhu et al. (2013).

All samples were stored in aerated seawater and transported to the experimental facilities within 4h. On both occasions, organisms were randomly distributed across four identical aquaria (100 x 45 x 70cm). These were equipped with a continuous flow-through mechanism, allowing the homogenisation of approximately 400L natural seawater in circulation per system. All aquaria were continuously aerated and pre-set at laboratory conditions mimicking the seawater salinity, temperature and pH at the time of sampling. After an initial acclimatisation period of minimum 48h under ambient conditions, both seawater temperature and pH were manipulated individually across the aquaria. This resulted in a 2x2 factorial design with four experimental treatments: a control treatment [CTRL: current temperature and pH], an ocean acidification treatment [OA: current temperature and lowered pH], an ocean warming treatment [OW: elevated temperature and current pH] and a combined climate change treatment [CC: combined elevated temperature and lowered pH]. Weekly, triplicated individual closed-core incubations were set up to measure N_2O emission by the mussel and by the microbial biofilm living on its shell. To distinguish between these two sources, whole mussels [*WHOLE*] and emptied mussel shells [*SHELL*] were

incubated separately, along with a control incubation. An additional control consisted of whole mussels in a 2% $ZnCl_2$ (50% w/v) - seawater solution to inhibit all biological activity [*ZNCL*]. Each incubation core held one individual or emptied shell and was kept at the correct temperature throughout the incubations. A magnetic stirrer ensured an evenly mixed water column in the cores throughout the 3h incubations. Discrete 30mL water samples were taken at the start and end of the closed-core incubations and fixed with 100μL saturated $HgCl_2$ solution for N_2O analysis. Quantification of dissolved N_2O was done by gas chromatography (SRI 8610C) and the N_2O emission rates (ER) of whole organisms and dissected shells were calculated according to equation 6:

Equation 6 $$ER\ (nmol\ ind^{-1}\ h^{-1}) = \frac{V\ (C_1-C_0)}{(t_1-t_0)}$$

with V the volume (L) of the incubation core corrected for the biovolume of the whole organism or shell and with C_0 and C_1 the concentrations of N_2O (nmol L^{-1}) at the start and finish of the closed-core incubation, t_0 and t_1 (h), respectively. After three and six weeks of manipulations [*WK3* and *WK6*, respectively], triplicated closed-core incubations with individual whole organisms were set up and sampled as described above. Along with N_2O emission rates (calculated according to 7), dissolved inorganic nutrients (DIN) were measured through discrete sampling (25mL; analyses performed by SKALAR SAN++) at the start and end of closed-core incubations with and without the addition of 20mM $NaClO_3$. DIN flux was calculated according to

Equation 7 $$ER\ (nmol\ g^{-1}DW\ h^{-1}) = \frac{V\ (C_1-C_0)}{g\ (t_1-t_0)}$$

Equation 8 $$DIN\ flux\ (\mu mol\ g^{-1}DW\ h^{-1}) = \frac{V\ (C_1-C_0)}{g\ (t_1-t_0)}$$

with parameters identical as in Equation and g the dry weight (g) of the mussel's soft tissue.

$NaClO_3$ inhibits the oxidation of nitrite (NO_2^-) to nitrate (NO_3^-) in the nitrification pathway (Belser & Mays 1980), and therefore the NCD pathway (7). Hence, all N_2O produced in this treatment is a result of nitrification (as a by-product during ammonium oxidation) or nitrifier denitrification (as a result of denitrification of nitrite (Tallec et al. 2008)), as well as through denitrification of nitrate already present in the incubation core.

In addition, three different labelled N-tracer treatments were set up to investigate the production of double-labelled $^{46}N_2O$ from either nitrification [*NIT*], nitrifier denitrification [*DNO2*] or nitrification-coupled denitrification [*DNO3*], in which NH_4^+, NO_2^- or NO_3^- act as a precursor to N_2O emission, respectively (**Error! Reference source not found.**; Fig. 6**Error! Reference source not found.**). The composition of these N-tracer treatments, in which ^{15}N was introduced using $^{15}NH_4Cl$ [*NIT*], $Na^{15}NO_2$ [*DNO2*] or $Na^{15}NO_3$ [*DNO3*], and the resulting concentrations in the incubation cores were identical to those in (Heisterkamp et al. 2013).

Table 1 Nitrogen tracer treatments NIT, DNO2 and DNO3 with the targeted N_2O-producing pathway and precursor, the concentrations of ^{15}N and ^{14}N added to the treatments and the possible combinations of ^{14}N and ^{15}N to form $^{45}N_2O$ and $^{45}N_2O$, respectively (from Voet et al. in prep)

	NIT	DNO2	DNO3
Pathway	Nitrification	Nitrifier denitrification	Nitrification-coupled denitrification
Precursor	oxidation of NH_4^+	denitrification of NO_2^-	denitrification of NO_3^-
^{15}N added	$^{15}NH_4^+$ (50µM)	$^{15}NO_2^-$ (50µM)	$^{15}NO_3^-$ (50µM)
^{14}N added	$^{14}NO_2^-$ (500µM)	$^{14}NO_3^-$ (500µM)	-
$^{45}N_2O$	$^{14}NH_4^+$/ $^{14}NO_X^-$ + $^{15}NH_4^+$	$^{14}NO_X^-$ + $^{15}NO_2^-$	$^{14}NO_X^-$ + $^{15}NO_3^-$
$^{46}N_2O$	$^{15}NH_4^+$ + $^{15}NH_4^+$	$^{15}NO_2^-$ + $^{15}NO_2^-$	$^{15}NO_3^-$ + $^{15}NO_3^-$

Before manipulations took place [*WK0*] and at *WK3* and *WK6*, triplicated closed-core incubations for all three N-tracers were set up in all experimental treatments. The 125mL incubation cores held one individual in seawater from its respective experimental treatment amended with the respective N-tracer, and were incubated for 4h on a shaking table to ensure adequate mixing. Hourly, 1mL samples were taken with a surgical syringe and transferred to 12mL He-flushed exetainers, prefilled with 100μL saturated $HgCl_2$ to fixate the N_2O and 37.4ppm unlabelled N_2O to ensure the detection limit of the mass spectrometer was reached. Since only 4% of the core volume was sampled by the end of the incubation, under-pressure was not an issue and the withdrawn volume was therefore not replaced. The concentrations of $^{45}N_2O$ and $^{46}N_2O$ (nmol L^{-1} g^{-1}DW) were calculated as described by Heisterkamp et al. (2013) after the samples were analysed by gas chromatography-isotope ratio mass spectrometry (GC-IRMS; Finnigan Trace GC Ultra). The linear increase of $^{45}N_2O$ and $^{46}N_2O$ over time was used to calculate net emission rates (nmol g^{-1}DW h^{-1}).

A vertical oxygen profile of the microbial biofilm on three replicate *M. edulis* shells was measured before manipulations started [*WK0*] and in each experimental treatment after three and six weeks [*WK3* and *WK6*, respectively]. Individuals were carefully dissected from their shell with a scalpel and dissected shells were placed in aerated seawater from the respective experimental treatments. A Unisense™ MicroProfiling System was used to position the sensor tip of a PyroScience™ fiber oxygen microsensor on the shell surface, and a vertical dissolved oxygen concentration profile was recorded in increments of 50 or 100μm through the biofilm to a distance of 3000μm from the shell surface. This was done at three random positions on the shell of each replicate organism in dark conditions. Finally, a multivariate matrix was constructed with the oxygen concentrations at each distance above the shell (Widdicombe et al. 2013).

Data analysis

We used linear mixed effects models to test the effect of temperature and pH on the emission of N_2O in the *WHOLE*, *SHELL*, $NaClO_3$-inhibited and non-inhibited incubations. Random factors included incubation core and/or experimental week. If none of the random factors explained left-over variance, a linear regression model was fitted. The effect of temperature, pH and

experimental week on DIN flux was analysed using linear regression models. Significance of the two-way interaction 'temperature x pH' and post-hoc pairwise comparison were used to identify possible interaction effects of temperature and pH. We checked normality of the residuals and model assumptions, Gaussian error distributions were used and model selection was either based on the parametric bootstrap and Kenward Roger methods for mixed model comparison (Halekoh & Højsgaard 2014) or on the backwards selection procedure for linear regression models. Statistical analyses were conducted using R v3.6.1 and RStudio v1.4.1106 (RStudio Team 2016; R Core Team 2019). Linear mixed effects models were built using the R package *lme4* (Bates et al. 2015) and linear regression models were fitted using the *stats* package (R Core Team 2019).

We used PERMANOVA to investigate differences in the shell biofilm oxygen microprofiles between treatments and weeks. All profiles on all shells were considered as replicates within the Euclidian distance matrix. Homogeneity of multivariate dispersion was tested for all significant PERMANOVA factors using PERMDISP tests. Pairwise tests were used for detailed investigation of significant terms. Finally, the SIMPER routine was used to identify which distances from the shell contributed most to any observed differences. Multivariate analyses were carried out in Primer v6.0 with PERMANOVA + add-on software (Clarke & Gorley 2006; Anderson et al. 2008).

3.2.4 Benthos experiments

3.2.4.1. Ocean acidification effects on the behaviour of two sediment ecosystem engineers (based on Vlaminck et al., subm. a).

Set-up

Behaviour is often one of the very first features of an animal's activity to respond to environmental stress. At the same time, many macrobenthic invertebrates exhibit behaviours which affect ecosystem processes that are key to benthic biogeochemistry. The white furrow shell, *Abra alba,* is a bivalve which randomly reworks the surface 2 cm of sediment in search for food, a behaviour often referred to as bio-diffusion (Gérino et al. 2003). Its feeding behaviour is, however, plastic, and can involve deposit feeding as well as suspension feeding (Holtmann et al. 1996). In the BPNS, this species attains densities up to 7000 individuals m^{-2} and is thé sentinel species of the most biodiverse communities inhabiting fine-sandy sediments (Degraer et al. 2006, Breine et al. 2018). The sand mason *Lanice conchilega* is a tube-building polychaete which, when present in high abundances, can form reef-like structures that enhance the deposition of suspended particulate matter, including food particles, and provide shelter against predation for a variety of benthic organisms (De Smet et al. 2015). *Lanice* flushes water through its tube and burrow, thus irrigating the sediment with oxygen-rich water. This behaviour is known as piston pumping (Forster et al. 1999). Like *A. alba*, it can switch between deposit feeding and suspension feeding, the former behaviour usually being the predominant one (Buhr 1976, Buhr & Winter 1977, Holtmann et al. 1996). Natural densities of *Lanice conchilega* in the study area reach up to 1000 ind. m^{-2} (Degraer et al. 2006). Both species are widely distributed and among the most abundant macrofauna in shallow waters of the North Sea (Seaward 1990, Van Hoey et al. 2008); because of their respective behaviours, they influence nutrient cycling and affect the abundance and community composition of meiobenthos, the small, diverse and highly abundant micro-invertebrates that inhabit aquatic sediments (Braeckman et al. 2010).

Here we investigate the behavioral response of both macrobenthos species to experimental ocean acidification. Since both species live inside sediments, observing their behaviour – particularly at a high temporal resolution – is far from evident. However, macrobenthos activities such as the above-described biodiffusion and bio-irrigation generate pressure waves in the sediment pore water. These hydraulic pressure waves can be measured using specially designed pressure sensors (Wethey & Woodin 2005, Volkenborn et al. 2010), thereby enabling permanent recording of an animal's behaviour in a sediment mesocosm. We used Honeywell type 26PC pressure sensors and fixed them into a plastic tube (Ø = 1.2 cm, height = 11.5 cm) with a sealed bottom and open top. Each sensor contained a pressure port close to the wall of the tube and a reference port in seawater plenum inside the tube (Wethey & Woodin 2005, Woodin et al. 2010). Sensors were all calibrated prior to their deployment.

Obviously, different activities of animals may cause different hydraulic pressure signals, so in order to be able to interpret specific behaviours from porewater pressure profiles, particular changes in porewater pressure have to be coupled to particular activities of animals. For *L. conchilega*, we focused on its piston-pumping behaviour, since this has major effects on sediment biogeochemistry, while for *A. alba*, we focused on its two different feeding behaviours, deposit feeding and filter feeding. In dedicated experiments preceding our work on the effects of acidification, we recorded porewater oxygen dynamics using microsensors (type ox25, Unisense) that were inserted into the sediment at a distance of 5 mm from a *L. conchilega* tube to record piston-pumping behavior (Foshtomi et al. 2018). Porewater hydraulic signatures were simultaneously recorded at a distance of ~ 2.5 cm from the tube using the pressure sensors. Pressure sensor data were smoothed to reduce noise (Wethey & Woodin 2005, McCartain et al. 2017). The synchronization of the porewater pressure and the oxygen data confirmed that the piston-pumping behavior could be clearly detected from hydraulic signatures (Fig. 9).

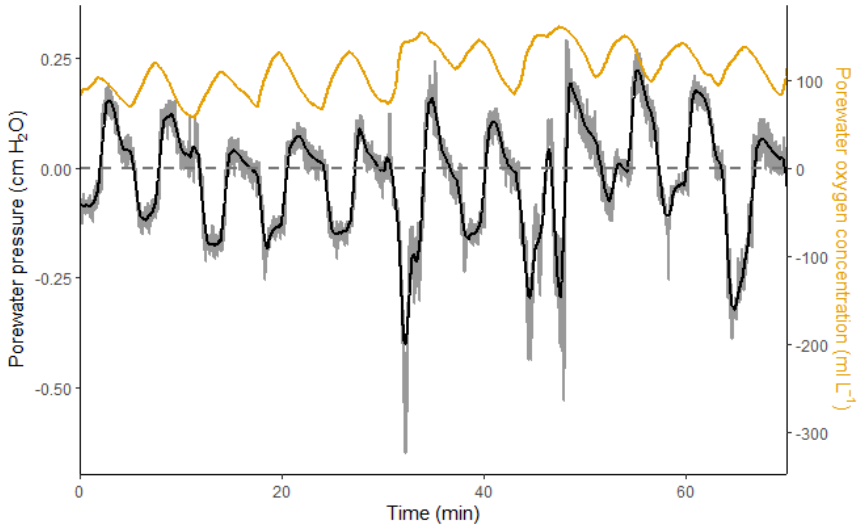

Figure 9 Visualisation of piston pumping behavior of L. conchilega *by the hydraulic signature of the porewater records (black) and the changes in oxygen concentration in porewater adjacent to the tube (orange).*

For *A. alba*, we mounted a GoPro (HERO 3+) camera in small experimental sediment arenas to which a single *A. alba* was added. The GoPro recorded movement and activity of the bivalve at the sediment surface at 1-sec intervals. We simultaneously measured porewater hydraulic signals using the same pressure sensors as for *L. conchilega*. The synchronization of the time-lapse imagery and the porewater pressure signals allowed us to identify the two types of feeding behaviour of *A. alba* (Figure 10), their duration and frequency (Figure 10.A and 10.B).

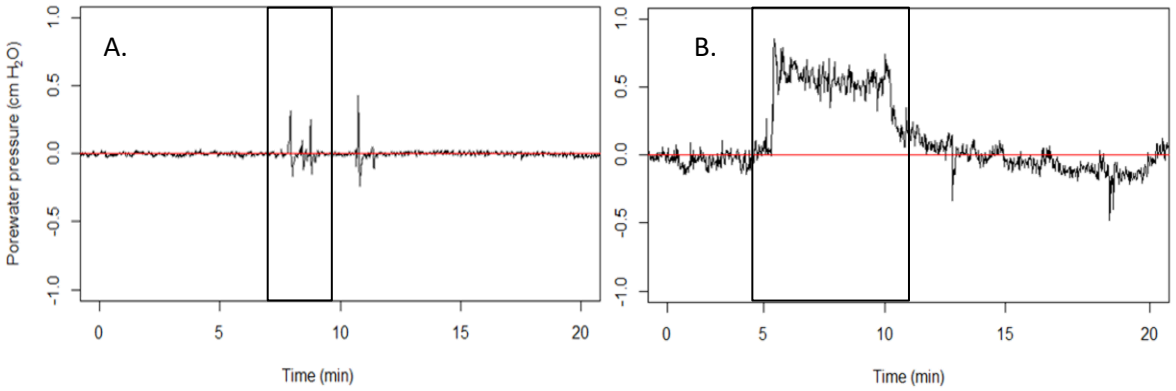

Figure 10 Hydraulic signatures associated with different A. alba behaviors: deposit feeding + defecation (A.) and filter feeding (B.). Waveforms are highlighted in a black frame.

Organisms were obtained from subtidal station 780 at the BPNS and from the intertidal at Heist for *A. alba* and *L. conchilega*, respectively, and left to acclimatize to lab conditions for two weeks, after which pH was decreased by 0.3 units in steps of 0.1 per day. The behavioral response to this OA was observed after two and four weeks of incubation for *L. conchilega* and *A. alba*, respectively. pH and temperature were logged every ten minutes with the IKS Aquastar system. In addition, temperature and pH were measured on a weekly basis using a portable pH/conductivity meter (Metrohm; Model: 914). Seawater samples were collected weekly from each incubation tank and filtered through Whatman GF/C filters for Total Alkalinity (TA) measurements on a HydroFIA TA (CONTROS Systems & Solutions GmbH) at the Flanders Marine Institute (VLIZ). CO_2SYS software (Pierrot et al. 2011) was used to derive carbonate chemistry parameters (pH_T, pCO_2, HCO_3^-, CO_3^{2-}, Ωc and Ωa) from the measured values for temperature, pH , salinity and TA.

There were eight microcosms per species, evenly spread over two incubation tanks (CTRL and OA), and containing one individual each. Behaviour of *L. conchilega* was measured with pressure sensors, that of *A. alba* with time-lapse imagery (see above).

Data analysis

The effect of pH (CTRL and OA) on total feeding time, feeding frequency and mean duration of a feeding event per feeding mode was investigated using t-tests. Possible differences in pumping frequency of *L. conchilega* between treatments (CTRL and OA) and over time (baseline, week 1 and week 2) were evaluated using two-way ANOVA with Tukey HSD pairwise comparisons in case of a significant ANOVA result. Data was $\log_{10}$ transformed to improve normality when indicated by Shapiro-Wilk tests. All statistical analyses were performed using R-software version 4.0.4 (R Core Team, 2014).

3.2.4.2. Ocean acidification reduces fitness of a benthic bio-engineer, the bivalve Abra alba *(based on Vlaminck et al., subm. b).*

Set-up

Here we build on the results of the previous study (3.2.4.1) where we focused on behavioral responses of two key species to ocean acidification. In this study, we complement the behavioral information on *A. alba* with detailed ecophysiological and bioenergetic responses, and we do this under two different potential future pH scenarios, i.e. the same one as in 3.2.4.1 (-0.3 units, RCP 4.5) and a stronger acidification (-0.5 units, RCP 8.5) in addition to an ambient pH (CTRL, $pH_T \sim 8.2$) treatment. Unlike in the previous experiment, we now incubated individuals at natural densities, and measured various physiological parameters and indicators of organism health after 3 and 5 weeks of incubation. We expected a higher energy allocation to physiological processes that mediate the impact of acidification, either compensated by a higher resource utilization or resulting in fitness loss. Given that a higher filter feeding activity, measured as the phytoplankton clearance rate, causes a higher ingestion of acidified seawater in OA treatments (Fernández-Reiriz et al. 2011), we rather expected alternative ways of increasing food uptake, either by increasing absorption efficiency and/or by shifting to deposit- instead of filter-feeding.

Sampling and acclimatization of experimental animals as well as the general experimental set-up were as described under 3.4.2.1. Temperature, pH, salinity and total alkalinity were measured and used to derive carbonate chemistry parameters (pH_T, pCO_2, HCO_3^-, CO_3^{2-}, Ωc and Ωa) via CO_2SYS software (Pierrot et al. 2011) as under 3.4.2.1. Mortality was checked daily, and dead organisms were removed but not replaced.

Measurements of *A. alba* physiology and condition were performed after 3 and 5 weeks of incubation. 16h before measurements, 6 animals were placed in 1.5-L incubation chambers to allow animals to empty their guts. 0.1 mL of Shellfish Diet 1800 was subsequently injected into the incubation chamber and homogenized through gentle stirring. At half-hourly intervals, 10-ml water samples were collected over a period of 3 h for quantification of algal cell density using a Coulter Multisizer. Algal clearance rates (CR) were estimated from the exponential decline in cell concentration using equation (9) (adapted from (Jacobs et al. 2015)).

$$CR\ (L\ g^{-1}DW\ h^{-1}) = \frac{V}{g*t} * (ln\frac{C_0}{C_t}) \quad (9)$$

Faeces produced during the 3-h incubation was collected and filtered over preweighed Whatman GF/C filters and rinsed with isotonic ammonium formate before drying to constant weight at 60 °C. Filters were then combusted at 450 °C for 3 h and weighed again to estimate organic and inorganic fractions of the faeces (Conover 1966). Samples of suspended algae were processed in the same way to estimate the organic fraction of the food, allowing calculation of the absorption efficiency (AE) as

$$AE\ (\%) = \frac{(F-E)}{(1-E)*F} * 100 \quad (10)$$

Where F is the ash-free dry weight : dry weight ratio of the food and E is the ash-free dry weight : dry weight ratio of faeces (Conover 1966). Finally, absorption rate (AR) was calculated as the

product of the organic ingestion rate (OIR) and AE, OIR in turn being the product of CR and the organic carbon content of the food.

$$AR\ (mg\ g^{-1}\ DW\ h^{-1}) = AE * OIR \qquad (11)$$

Respiration rates (RR) were measured as described under 3.2.2, using equation 3 in that section.

Estimates of excretion rates (see equation 12 (Magni et al. 2000)) used the differences in concentrations of ammonia, nitrogen and phosphate at the start and end of each closed-core incubation. These concentrations were determined via Continuous Flow Analysis on a Skalar San^{++} after sample filtration through Whatman GF/C filters. Total alkalinity of similarly filtered water portions was determined via titration using a HydroFIA TA (CONTROS Systems & Solutions GmbH) at the Flanders Marine Institute (VLIZ).

$$ER\ (\mu mol\ g^{-1}\ DW\ h^{-1}) = \frac{V*(C_0-C_1)}{g*(t_1-t_0)} \qquad (12)$$

where V is the volume of seawater in the incubation chamber, C_0 and C_1 are the ammonia concentrations (μg/L) at the start and end of the incubation, respectively, g is the total soft tissue dry weight of the organisms (g), and t_0 and t_1 are the start and end time of the incubation, respectively (h).

Estimates of calcification rate followed the alkalinity anomaly method (Gazeau et al. 2015). Seawater samples of 50 mL were taken at the start and end of the incubation period and analyzed for total alkalinity (see above).

$$Calcification\ rate\ (\mu mol\ g^{-1}\ DW\ h^{-1}) = \frac{\Delta NH_4^+ - \Delta TA - \Delta NO_x - \Delta PO_4^{3-}}{2*g*(t_1-t_0)} \qquad (13)$$

where t_0 and t_1 are the time (h) at the start and end of the incubation, respectively; g is the soft tissue dry weight (g) of the animals in the incubation chambers; and ΔTA, ΔNH_4^+, ΔNOx and ΔPO_4^{3-} (in µmol kg^{-1}) are the differences in total alkalinity and in the concentrations of ammonium, nitrate plus nitrite, and phosphate between the start and end of the incubation.

A scope for growth (SFG) was estimated from the above physiological parameters (Warren & Davis 1967) (equation 14).

$$SFG\ (J\ g^{-1}\ DW\ h^{-1}) = A - (R + U) \qquad (14)$$

Where A represents the absorbed energy and thus equals C * Absorption Efficiency, with C being the consumed energy (C = clearance rate * microalgal biomass * microalgal energy equivalent). R represents the respiratory energy loss (R = respiration rate * energy equivalent O_2) and U the energy loss through excretion (U = excretion rate * energy equivalent ammonia). The energy equivalents used were: 1 µmol O_2 = 0.456 J (Gnaiger 1983), 1 µmol NH_4–N = 0.349 J (Elliott & Davison 1975), 1 g DW algal food = 1004.16 J (Reed Mariculture Inc.).

Finally, the six animals that were used for physiological measurements were placed on the sediment surface of a separate container and the time until full burial was measured as a proxy for animal condition (Rodríguez-Romero et al. 2014).

Data analysis

Differences in furrow shell survival between acidification treatments were analyzed using Permutational Multivariate Analysis of Variance (PERMANOVA) (Anderson 2017). The effects of OA and time on the condition index and physiological parameters of *A. alba* were assessed using two-way analysis of variance (ANOVA) with Tukey HSD post-hoc tests. The effect of OA on furrow shell calcification rate (measured only after 3 weeks) was analysed using one-way analysis of variance (ANOVA), while differences in burial speed between treatments and times (after 3 and 5 weeks of incubation) did not meet the assumptions of parametric tests and were therefore analysed using two-way PERMANOVA. All statistical analyses were performed in R version 4.0.4 (R Core Team, 2014).

3.2.4.3. Ocean acidification and warming effects on the faunal stimulation of sediment biogeochemistry (based on Vlaminck et al., in prep.).

Organisms and sediment were collected as described in 3.2.4.1. A system of paired tanks, consisting of one incubation tank (120 L) and one holding tank (80 L), was set up. To mimic natural conditions, the incubation tanks were aerated and water flow between the incubation and holding tank was established. Every week, 30 L of seawater was refreshed to avoid nutrient build-up and maintain ambient salinity. The tanks were kept in a temperature controlled room in a 12:12 h light:dark regime.

Experimental set-up and seawater manipulation

Two experiments were conducted (Fig. 11): one with *Abra alba* (experiment 1), one with *Lanice conchilega* (experiment 2). 32 Plexiglas cores (10 cm internal diameter) were used in each experiment.

Figure 11. Experimental set-up in the laboratory: full set-up with large tanks and pressure sensor monitoring on a laptop (left) and details of pressure sensor application in microcosms with Abra alba *(middle) and* Lanice conchilega *(right).*

All cores were filled with sieved and homogenized sediment up to approximately 10 cm below the rim and distributed randomly over 16 tank-systems. After a sediment settling and acclimation time of 7 weeks, *A. alba* (experiment 1) or *L. conchilega* (experiment 2) individuals were added to one core in each tank, at natural densities (*A. alba*: n = 9, *L. conchilega*: n = 6 per core) (Van

Hoey et al. 2014). Sediment and organisms were exposed to manipulated conditions for 6 weeks. A fully crossed experimental design with two factors was applied, with temperature (ambient or elevated) and pH (ambient or lowered) each with two levels, to investigate the effects of climate change on macrofauna and their effect on sediment biogeochemistry. After one (*L. conchilega*) and two weeks of acclimatization (*A. alba*) to ambient conditions, seawater pH was lowered by 0.1 unit per day and temperature was elevated by 1 °C per day over a period of three days. Manipulation of seawater pH (-0.3 units) and temperature (+3°C) was done as described in the general approach (see above). Organisms were fed twice a week with 5 mL of commercial Shellfish Diet 1800 (Reed Mariculture Inc., composed of 40 % *Isochrysis*, 15 % *Pavlova*, 25 % Tetraselmis and 20 % *Thalassiosira weissflogii*) diluted in 16 L of seawater and distributed equally in the 16 tanks. Seawater carbonate chemistry parameters were monitored weekly as described above. Mortality was checked daily and dead organisms (*L. conchilega:* n = 2, *A. alba:* n = 61) were removed to avoid nutrient build-up.

Flux measurements and sampling

After three and six weeks of incubation in each experiment, the Sediment Community Oxygen Consumption (SCOC) and nutrient exchange at the sediment water interface were quantified, through closed, dark incubations of the cores. Sediment cores were closed airtight, allowing us to measure changes in oxygen and nutrient concentration in the water column (approximately 10 cm). The overlaying sea water was mixed with a motorized stirrer built into the lid, to avoid stratification of the water column. The mixing rate was kept low enough to avoid resuspension of the sediment. Oxygen concentration in the overlaying sea water was continuously monitored with Robust Oxygen Optodes (OXROB 10, Pyroscience sensor technology), connected to an optical oxygen meter (FirestingO2, Pyroscience). Incubations were run for 3 h, long enough to measure changes in oxygen and nutrient concentrations, while the oxygen concentration of the seawater remained above 60 % saturation. Discrete water samples (10 mL) were taken and filtered through Whatman GF/F filters at the start and end of the closed incubation to determine nutrient concentrations.

Oxygen fluxes were calculated from the slopes of the linear regression of oxygen concentration over time. Nutrient fluxes were calculated as the difference between the nutrient concentrations at the end and start of the incubation.

Oxygen microprofiles were measured in the sediment after 5 weeks of incubation. Oxygen microsensors (Unisense OX100, 100 μm tip size) were vertically inserted into the sediment and moved with a Unisense microprofiler at increments of 250 micrometer (two replicate profiles in each core). SensorTracePro software (Unisense) was used to visualize the output. The O_2 microsensor was 2-point calibrated with a 0% oxygen solution (Na-ascorbate solution) and a 100% oxygen solution.

Nitrification, denitrification and total carbon and nitrogen mineralization were estimated using the sediment-water exchange fluxes of O_2, NO_x and NH_x. A mass budget of oxygen, nitrate and ammonium in the sediment was constructed as a function of source and sink processes (Soetaert et al. 2001, Braeckman et al. 2010).

Data Analysis

Differences in survival of study organisms between treatments were analyzed using two-way analysis of variances (ANOVA) with temperature and pH as fixed factors, with two levels each (ambient and increased temperature; ambient and lowered pH). If significant effects were found, Tukey HSD tests were performed to identify pairwise differences. To test the effect of *Abra alba* or *Lanice conchilega* (present or absent), climate (ambient, low pH and high temperature), time (three or six weeks of incubation) and their interaction effects on biogeochemical fluxes, linear mixed effects models were constructed for each response variable (organism presence, climate and time). We allowed random intercepts for tank identity to take the non-independence of the two cores in each tank into account. Step-by-step deletion of single model terms that were not engaged in a significant interaction led to the minimal adequate model. The Kenward-Roger method was used to estimate degrees of freedom, calculate F-statistics and associated p-values. Model assumptions were checked graphically, the normality of residuals was numerically confirmed with a Shapiro-Wilk test. Statistical analysis was conducted in R-software version 4.0.4 (R Core Team, 2014) with packages *lme4* (Bates et al. 2014), *lmerTest* (Kuznetsova et al. 2017) and *MuMIn* packages (Barton 2020).

3.2.5. Molecular approach

Sample collection and treatment

Animals and empty shells for the study of climate change effects on the mussel microbiome and its possible involvement in N_2O production were obtained from the experiment with fouling fauna described under 3.2.3. We therefore do not repeat information on the (pre)treatment of the experimental animals here, nor on the experimental design and incubation conditions.

We used a direct flux approach to determine the aerobic respiration rate of microbial biofilms on the shells of blue mussels. In short, three living mussels per experimental microcosm were opened by cutting the posterior adductor muscle, followed by the complete removal of all soft tissues, leaving us with empty mussel shells and their epimicrobiome. These shells were placed one by one in incubation chambers filled with water from their respective mesocosms. Each incubation chamber was maintained at the temperature corresponding to the associated experimental treatment. Chambers were then sealed and O_2 in the water column was measured using an OXROB10 oxygen probe (PyroScience) introduced through the mesocosm's lid. Water was homogenized by permanent stirring. Oxygen concentrations were determined at the start of the incubation and after 3 h, and aerobic respiration calculated as the decrease in O_2 concentration divided by the incubation time.

The contribution of microbial biofilms to dissolved ammonium (NH_4^+), nitrate (NO_3^-), nitrite (NO_2^-) and nitrous oxide (N_2O) concentrations were measured during the respiration incubations as described under 3.2.3.

We set out to determine both the (shifts in) composition of the epimicrobial biofilms growing on the shells, and to get an idea of their functional involvement in the N-cycle. For the latter purpose, we tried to optimize protocol for the quantification, using qPCR, of four key genes involved in essential steps of the N cycle. However, these attempts were only partially successful and did not

yield sufficiently reliable results. We therefore focus here on the epimicrobiome composition and its structural and possible functional shifts following climate change.

Metabarcoding of the mussel shell microbiome

Microbial biofilms were scraped from the shell surface of frozen mussels using sterile tweezers and razors. Total DNA was extracted using the phenol-chloroform procedure and mechanically homogenized before being centrifuged for 5 min (10,000 rpm at 4°C). Supernatant was resuspended in chloroform:isoamylalcohol (25:24:1 v:v:v), shaken and again centrifuged for 5 min; this step was repeated twice before the supernatant was transferred into a solution of 50 μL sodium acetate (3 M), 1 mL ethanol (EtOH 96%) and 2 μL glycogen (20 mg mL^{-1}) and incubated overnight at -20°C while permanently being mixed. Samples were then centrifuged, and the supernatant discarded, after which 1 mL of ethanol (70%) was added. This suspension was subsequently centrifuged twice to ensure complete removal of the ethanol. The remaining DNA-pellets were air-dried, resuspended in TE buffer (10mM Tris – 1 mM EDTA) and incubated for 20 min at 55°C to allow complete dissolution of the DNA pellets. DNA extracts were then stored at -20°C pending PCR amplifications.

In parallel to the mussel shell samples, 25-mL water samples of each experimental mesocosm were collected and filtered on a 0.2 µm polycarbonate membrane filter (Whatman™ 110606 Nucleopore™ Track-Etched). DNA extraction and purification followed the same protocol as for the microbial biofilms.

Bacterial and Archaeal epimicrobiomes were investigated using metabarcoding of the amplified V4 regions of the 16S small-subunit rRNA gene (using the primer pair 515F–806R) (Caporaso et al. 2011). Each sample was amplified in three technical replicates. Reverse primers contained a unique identifier for each sample and an Illumina adapter (Caporaso et al. 2011). Amplified PCR products were analyzed by electrophoresis. The technical replicates of amplified PCR products were pooled per sample before being purified using the Agencourt AMPure XP PCR Purification kit (Beckman Coulter). DNA quality was measured using a Qubit 3.0 fluorometer (Thermo Fisher Scientific). 10 ng of amplicon DNA of each sample was finally pooled, and the library was sent to Edinburgh Genomics, University of Edinburgh, for Illumina MiSeq sequencing using a 2 x 300-bp paired-end protocol.

Downstream analysis

Downstream analysis used the DADA2 pipeline (Callahan et al. 2016) in QIIME 2 (v.2019.4; (Bolyen et al. 2019) after removal of forward and reverse primers from the reads. Low-quality read portions (quality scores < 20) and chimeric sequences were removed. *Amplicon sequence variants* (ASV, Callahan et al., 2017) instead of operational taxonomic units (OTU) were used. We constructed a table with the frequency of each ASV in each sample, and with a taxonomic assignment of each ASV based on the SILVA 132 database (Quast et al. 2012). All ASVs with a frequency of less than 0.1 % of the minimum sample depth were removed, and so were sequence variants that could not be assigned a bacterial or archaeal taxonomy (these are generally mitochondrial and chloroplast 16S sequences).

QIIME 2 output files were analyzed using R v.3.6.2 (2019-12-12) (R Core Team 2019) with the "phyloseq" (McMurdie & Holmes 2013), "vegan" (Oksanen et al. 2019) and "GUnifrac" (Chen et

al. 2012) packages. For all analyses, data were first rarefied down to the smallest number of sequences detected in any sample, i.e. 24,658. Species richness, Shannon-Wiener diversity and evenness were calculated to cover different aspects of *microbiome α diversity*. We also identified the *core microbiomes* of mussel biofilms and water samples as composed of those ASVs that were shared by at least 90 % of mussel or water samples, respectively (Shade & Handelsman 2012).

While the above analysis allowed the comparison of α diversity and composition of the microbial biofilms, we also wanted to add a *functional profile* to this structural characterization of microbial communities. For this purpose, we used a "*phylogenetic investigation of communities by reconstruction of unobserved states*" approach (PICRUSt) using PICRUSt2 (Douglas et al., 2019; Langille et al., 2013). The unrarefied ASV table was used as input. Using the prediction table based on the Kyoto encyclopedia of genes and genomes (KEGG), we identified genes predicted to be involved in the nitrogen cycle (https://www.genome.jp/kegg/pathway/map/map00910.html). These genes and the pathways they are involved in comprise: assimilatory nitrate reduction (K00360, K00366, K00367, K00372), denitrification (K00368, K15864, K04561, K02305, K00376), dissimilatory nitrate reduction (K00367, K00372, K00360, K00366, K00362, K00363, K03385, K15876), dissimilatory nitrate reduction/denitrification (K00370, K00371, K00374, K02567, K02568), nitrification (K10944, K10945, K10946, K10535) and nitrogen fixation (K02588, K02586, K02591, K00531).

Data analysis

The influence of climate (four levels: control, acidification, warming, climate change (i.e. acidification + warming)) and sample type (two levels: mussel shell epimicrobiome vs water) on alpha diversity (richness, Shannon-Wiener diversity, evenness) and on the proportion of the microbiota belonging to the core microbiome was investigated using two-way analysis of variance (ANOVA) after checking the data for normal distribution and homogeneity of variances. If necessary, data were log-transformed to meet these assumptions. In case of a significant overall ANOVA result, Tukey HSD pairwise comparisons were performed to identify the pairs of 'treatments' between which significant differences existed. All analyses were performed with the free computing environment R (R Core Team 2019).

In order to compare effects of the same two factors as above, but now on biofilm community composition, we ran Permutational multivariate analysis of variances (PERMANOVA) (Anderson 2001); PERMDISP was used to assess multivariate dispersion (Anderson 2006). The effects of climate treatment and sample type were visualized using principal coordinate analysis (PCoA) based on generalized UniFrac distances (Chen et al. 2012). The software PRIMER® (v.6) with the PERMANOVA+ add-on software was used for these analyses of microbiome community composition.

3.3 Climate change experiments at the community level

A mesocosm experiment was conducted to mimic the OWF AHS colonising community under three different climate scenarios: control (CTRL: current temperature and pH), climate change (CC: elevated temperature and lowered pH) and climate change with multifunctional co-use of OWF and aquaculture activities (CC+AQ: elevated temperature, lowered pH and increased *M.*

edulis biomass). To track organic matter assimilation into the OWF faunal biomass, ^{13}C labelled microalgae (*Isochrysis galbana*) were added to the mesocosms. We tested the following hypotheses: (H1) a significant difference in biomass-specific and total carbon assimilation between OWF AHS colonising species, (H2) a significantly different biomass-specific carbon assimilation in the different climate scenarios, and (H3) a lower biomass-specific carbon assimilation in the CC + AQ mesocosm due to increased competition in the presence of blue mussel (*M. edulis*) aquaculture.

Organism and sediment collection

In September 2018, hard substrate fauna, natural sediment (incl. infauna) and mobile predators were collected on or near the C-Power OWF of the Thornton Bank, approximately 30 km off the Belgian coast.

The sampled hard substrate fauna consisted of *M. edulis*, scraped from the D6 turbine in the C-Power OWF (51°33.04'N - 02°55.42'E), and colonised PVC panels (15 x 15cm) harvested from the 'Artificial Hard Substrate Garden' (ASHG) (see 3.1).

Natural *in situ* sediment and associated infauna was collected using multiple Van Veen grabs (surface area 0.1 m^2). Sediment containers (Ø 0.6m x h 0.3m) were immediately filled with this unsieved sediment, preserving the whole sediment community. Each container held approximately 0.07 m^3 of natural sediment. Mobile predators were collected by bottom trawling in the proximity of the C-Power OWF and a selection of the starfish *Asterias rubens*, the sea urchin *Psammechinus miliaris* and the swimming crab *Liocarcinus holsatus* were handpicked. All hard-substrate organisms, mobile predators and sediment communities were stored in aerated seawater and transported to the experimental facilities within 4 h.

Experimental mesocosm set-up

Hard-substrate organisms and natural sediment were placed in three mesocosm systems, while mobile predators were temporarily incubated in two separate aquaria to avoid an excessive predation pressure on the AHS community at the start of the experiment. These separate aquaria were manipulated according to the same control (CTRL) and climate change (CC) regimes as the three mesocosm systems (*see below*). Each mesocosm system consisted of a large cylindrical holding tank (Ø 2.2 m x h 1.4 m) equipped with a temperature-controlled continuous flow-through mechanism with a total of ± 4000 L in circulation. Water column mixing and natural currents were mimicked using four separate inflow locations in each mesocosm. Predator incubation systems were similar, with two aquaria containing the organisms (0.6 x 1.0 x 1.4 m) and a ±1000 L temperature-controlled continuous flow-through mechanism on each aquarium. Both the mesocosm and predator incubation systems were aerated and filled with natural seawater at pre-set laboratory conditions, mimicking the seawater salinity, temperature and pH at the time of the experiment (34 PSU, 19 °C and pH 7.96; LifeWatch Belgium 2015). All systems were subjected to a 12:12 h light/dark regime, mimicking natural diurnal light variations at the seawater surface.

The three mesocosms mimicked three different environments through manipulation of seawater temperature, pH and/or the standing stock of *M. edulis*: a control environment (CTRL: current temperature and pH), a climate change environment (CC: elevated temperature and lowered pH)

and a climate change with aquaculture environment (CC+AQ: climate change conditions with additional *M. edulis*). Each mesocosm contained four 'OWF systems' (Figure 12), mimicking an OWF foundation with vertical zonation of colonising fauna and a sediment community at the bottom. Each 'OWF system' consisted of four elements: a PVC ladder with (1) a gridded *M. edulis* basket at the top, (2) a colonised AHS panel from the mid-water AHSG mooring in the middle, (3) a colonised AHS panel from the bottom mooring at the bottom of the ladder and, underneath the ladder, (4) a sediment container with natural sediment communities. In the CC+AQ mesocosm, each 'OWF system' had an additional PVC ladder with three gridded *M. edulis* baskets alongside it (Figure 1 right). Across all mesocosms, each *M. edulis* basket contained approx. 40 individuals, mimicking the relative AHS community densities at the location of sampling.

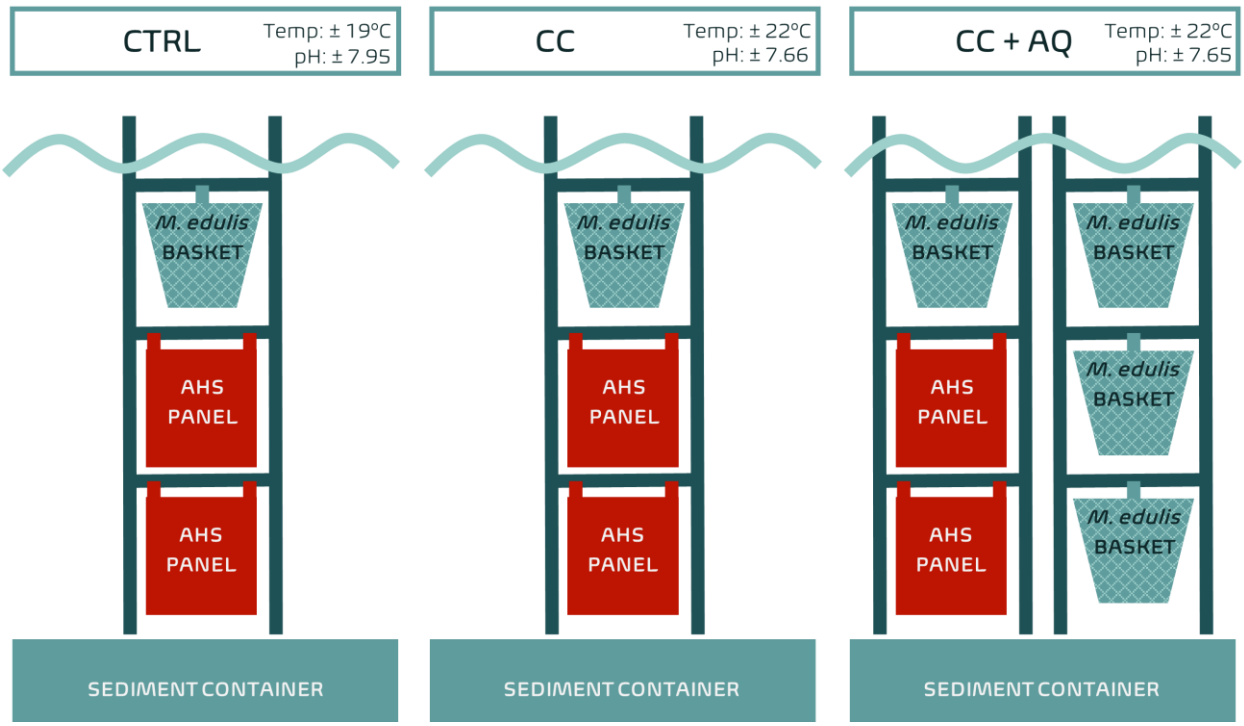

Figure 12 – schematic overview of 'OWF systems' (4 in each mesocosm) with a M. edulis *basket, two AHS panels and a sediment container in the CTRL and CC configuration (left and middle, respectively) and with 3 additional* M. edulis *baskets in the CC+AQ configuration (right).*

After an acclimatisation period of two weeks under ambient conditions, seawater temperature and pH were manipulated gradually over a period of six days (+1 °C and -0.1 pH unit in each step), resulting in seawater of +3 °C and -0.3 pH units (conform IPCC RCP 8.5 predictions) in both CC environments compared to the CTRL environment. These conditions were maintained for 46 days. Seawater temperature was regulated using Aqua Medic Titan 8000 professional units (mesocosm systems) or TECO TK2000 heaters (mobile predators) and pH was manipulated through the controlled bubbling of 100% CO_2 in the incubation tanks. Using JUMO (mesocosm systems) or IKS (mobile predators) temperature sensors and glass pH electrodes, all temperature and pH data was monitored, logged and manipulated automatically using a personalised Fleuren&Nooijen JUMO microprocessor (mesocosm systems) or an IKS AquaStar aquaristic computer system (mobile predators). Carbonate chemistry parameters were calculated as described in the general approach above.

All organisms were allowed to acclimatise to manipulated conditions for 34 days and were fed three times a week by adding 40 mL or 100 mL Shellfish Diet 1800® (Instant Algae® mix by Reed Mariculture Inc.) to the CTRL and CC or CC+AQ mesocosms, respectively, and by adding juvenile *M. edulis* individuals and ± 20 g Marine Mix (RUTO frozen fishfood®) to the mobile predator aquaria. During this acclimatisation period, two replicated closed-core incubations were performed weekly to measure sediment community oxygen consumption (SCOC) in each mesocosm as described in section 3.2.4.3.

The acclimatisation period was followed by a background sampling event (day 34) to establish a reference dataset of natural stable isotopes in the different OWF systems. This was done by sacrificing one 'OWF system' from each mesocosm (with accompanying aquaculture system in CC+AQ) and collecting, identifying and storing (-20 °C) all organisms attached to or associated with it. Additionally, 0.3 L seawater was filtered and sediment was sampled (both stored at -20 °C) in each mesocosm as well. At this point (day 34), the ^{13}C labelled *Isochrysis galbana* stock was added to each mesocosm (*see below*). An additional two 'OWF systems' were sacrificed from each mesocosm five days after the labelled algae addition (day 39), after which the (manipulated) mobile predators were added to the CTRL and manipulated mesocosms, respectively. The abundances of these predators were in line with approximated relative natural densities, mimicking a natural OWF environment (10 *A. rubens*, 4 *L. holsatus* and 8 *P. miliaris* per mesocosm (De Mesel et al. 2013, De Backer et al. 2020) and the delayed introduction of mobile predators was implemented to ensure a sufficient carbon assimilation in lower trophic levels before including the higher trophic levels in the mesocosm. The final 'OWF system' in each mesocosm was sampled 12 days after the addition of the labelled algae (day 46).

Labelled algae

The microalgae *Isochrysis galbana* was cultured at 23 °C under continuous light in autoclaved seawater supplemented with NutriBloom medium (PhytoBloom) and 10 g Sodium bicarbonate (99% ^{13}C) was added to a 60 L *I. galbana* stock. The microalgae culture was allowed to grow until even distribution across the three mesocosms would create the desired algal density of ± 145 mg C m^{-3} in each mesocosm, mimicking the annual mean phytoplankton biomass close to the Thornton Bank (Baretta-Bekker et al. 2009). The labelled microalgae had reached a mean fractional abundance of $a^{13}C = 0.0585$ when they were added to the experimental mesocosms, corresponding to a total of 253 mg ^{13}C added to each mesocosm.

Laboratory analysis

Before stable-isotope analysis, all 'OWF system' samples (including sediment and seawater filters) were oven-dried at 60 °C for 48 h. Dried organisms were weighed and grounded with a pestle and mortar to a fine homogenous powder. Subsequently, subsamples of ± 100 μg organic carbon were weighed in silver or tin cups (5-8 mm, Elemental Microanalysis UK) for organisms with or without a calcareous skeleton, respectively. After addition of 10 μL milli-Q® water, the silver cups were placed in a desiccator with HCl vapour (± 50 mL 37 % HCl) for 24 h to remove the calcareous fragments' carbon. Subsequently, all subsamples were oven-dried at 60 °C for 24 h.

Grounded organisms were standardly encapsulated individually, or multiple individuals of the same species, sampled in the same mesocosm at the same time, were pooled together when subsample weight was not sufficient. Stable Isotope Analysis (SIA) was performed at the Isotope

Bioscience Laboratory (ISOFYS, Ghent University, Belgium). Carbon isotopic composition was analysed using an ANCA-GSL elemental analyser interfaced with a 20-22 IRMS (SerCon, Cheshire, UK). Isotopic samples were measured relative to laboratory standards (adjusted to sample size) and a quality analysis (QA) sample was run every ten samples. ^{13}C normalisation (± SD) to Vienna Pee Dee Belemnite (VPDB) standard scale was done using WHEAT IA-R001 ($\delta^{13}C_{VPDB}$ = -26.43 ± 0.08 ‰, calibrated by Iso-analytical towards IAEA-CH6) and an in-house QA reference (Sorghum $\delta^{13}C_{VPDB}$ = -13.78 ± 0.17‰). Average analytical standard deviation on the δ value was determined by measuring five replicates of a sample of alanine ($\delta^{13}C_{VPDB}$ = -25.16 ± 0.20‰). For the enriched samples, the QA reference was a ^{13}C-enriched maize sample ($\delta^{13}C_{VPDB}$ = 396.9 ± 0.37‰).

Carbon assimilation

Isotopic composition $\delta^{13}C$ (standard delta notation in parts per thousand, ‰) of any sample was expressed as the carbon isotopic ratio (^{13}C:^{12}C) of a given sample ($^{13}R_{sample}$) relative to the Vienna Pee Dee Belemnite standard (VPDB) with $^{13}R_{VPDB}$ = 0.0111802, where

$$\delta^{13}C = \left[\frac{^{13}R_{sample}}{^{13}R_{VPDB}} - 1\right] * 1000$$

Carbon assimilation was calculated as the excess fractional abundance of ^{13}C ($a^{13}C$) in the sampled organism divided by the excess $a^{13}C$ of the labelled algae ($a^{13}C$ of natural *I. galbana* from Breteler et al. 2002). Excess $a^{13}C$ is the $a^{13}C$ of the sample above that of the non-enriched background, with

$$a^{13}C = \frac{^{13}R}{^{13}R+1} = \frac{^{13}C}{C} \approx \frac{^{13}C}{^{12}C+^{13}C} \quad \text{and}$$

$$\text{Carbon assimilation } [\mu gC\ \mu gC^{-1}_{biomass}] = \frac{a^{13}C_{sample} - a^{13}C_{background}}{a^{13}C_{labelled\ algae} - a^{13}C_{natural\ algae}}$$

Individual carbon assimilation [μgC ind^{-1}] was subsequently calculated by correcting the carbon assimilation for the carbon content of each sample [m%] and further multiplying it by the species-specific mean biomass of one individual [$\mu g_{biomass}$ ind^{-1}]. Such an individual carbon assimilation was calculated for each sample and subsequently averaged per species, sampling event and mesocosm.

To assess mesocosm carbon budgets, the mean individual carbon assimilation [μgC ind^{-1}] of each macrofauna species was multiplied by its abundance [ind] to estimate the total carbon assimilation [μgC] of each species in each mesocosm.

Data analysis

A non-parametric approach (Kruskal-Wallis Rank Sum test) was used to test for (1) differences in mean carbon assimilation between species within a mesocosm, (2) differences in mean carbon assimilation between experimental mesocosms within a species, and (3) differences in total carbon assimilation. This choice was made based on an unbalanced dataset and high kurtosis of the isotopic data. Species with less than 3 subsample replicates per sampling event or

experimental mesocosm were excluded from analysis. The Dunn's Kruskal-Wallis Multiple Comparisons test (KWMC, with Bonferroni correction) was used for post-hoc analysis of differences. SCOC measured in each mesocosm was compared using one-way ANOVA and Tukey's HSD post-hoc test. SCOC data were normally distributed and homogeneity of variances was verified using Levene's test. All statistical analyses were handled at the 5% significance level and conducted using R Studio software version 1.4.1106 (RStudio Team 2016).

3.4 Ecological modeling

We implemented an experiment-based ecological model by integrating three submodels: (1) a physical (hydrodynamic *k-ε*) submodel driven by atmospheric forcings such as wind speed, air temperature and solar radiation; (2) a pelagic biogeochemical submodel, subjected to the hydrodynamically modelled water temperature and turbulence; and (3) a biological submodel of AHS colonising fauna model species *Mytilus edulis*, *Jassa herdmani* and *Metridium senile*.

The final ecological model (Fig. 13) described a marine NPZD$_2$ model (based on Meire et al. 2013 and De Luca et al. 2016), including one OWF turbine foundation with an AHS colonising community (represented by the three OWF AHS model species mentioned above), a *M. edulis* longline aquaculture set-up (design based on Buck et al. 2010) and the additional emission of nitrous oxide (N_2O) by *M. edulis* and its associated shell biofilm (see section 3.2.3). The model was built and implemented in R v3.6.1 with RStudio v1.4.1106 (RStudio Team 2016; R Core Team 2019) and solved with the *ReacTran* package (Reactive Transport Modelling in 1D, 2D and 3D; (Soetaert & Meysman 2012) to describe reaction and advective-diffusive transport models in aquatic systems.

The model was run for five years and the OWH AHS colonising fauna biomass, the *M. edulis* aquaculture biomass and the emission of N_2O by *M. edulis* and its associated shell biofilm was compared between all possible combinations of the model scenarios described below.

Climate scenarios

Four different climate scenarios were modelled: a control scenario [CTRL] with current seawater temperature and pH, an ocean acidification scenario [OA] with current seawater temperature and lowered pH, an ocean warming scenario [OW] with elevated seawater temperature and current pH and a combined climate change scenario [CC]. The ecophysiological parameters of *M. edulis*, *J. herdmani* and *M. senile* in these four scenarios were recalculated from the experiments reported in sections 3.2.2 and 3.2.3 . The climate conditions in these experiments were based on IPCC RCP 8.5 predictions for ocean warming and acidification towards the end of this century, with a rise in seawater temperature of 3°C (20°C vs. 23°C) and a drop in oceanic pH of 0.3 (7.66 vs. 7.96) (Hoegh-Guldberg et al. 2014). To ensure conformity between the use of ecological parameters with a T_{ref} of 10°C and the use of ecophysiological experiments at a higher temperature, the Q_{10} temperature dependency formulation of the feeding, respiration and mortality rates, as well as the temperature dependent N_2O gas transfer velocity, was adjusted to incorporate a T_{ref} of 20°C or 23°C, respectively. Apart from the adjusted ecophysiological parameters and temperature dependency, all other parameters and biogeochemical or biological processes were identical.

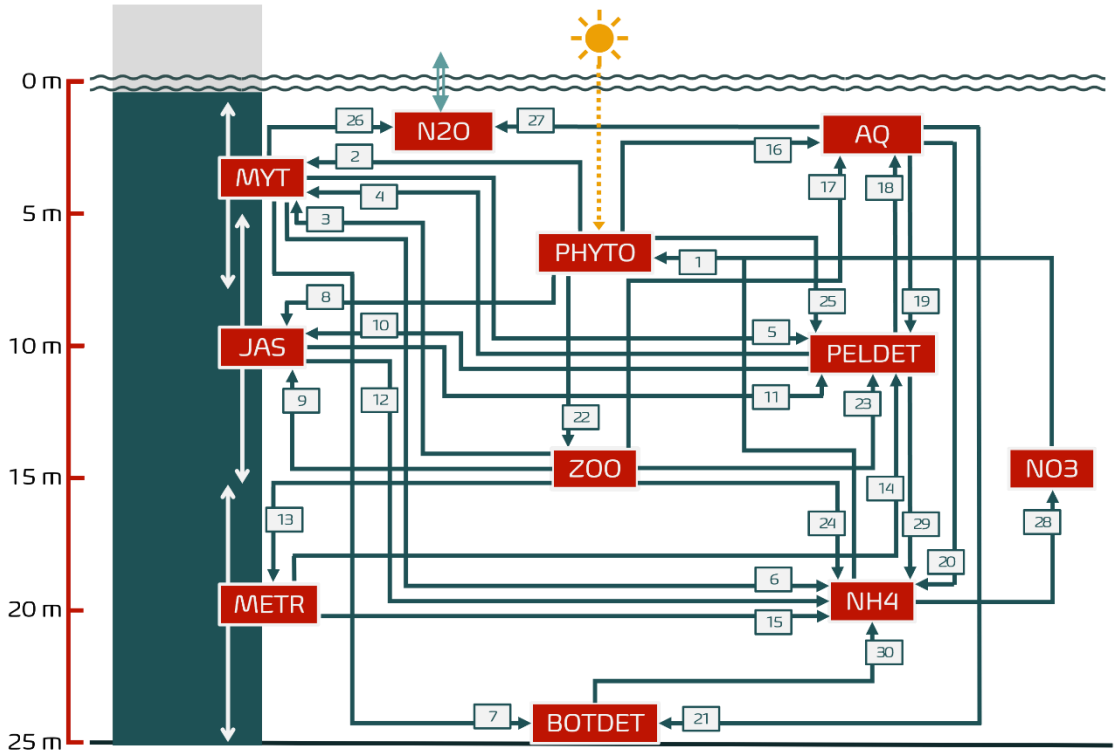

1: Primary production
2: PHYTO uptake by MYT
3: ZOO uptake by MYT
4: PELDET uptake by MYT
5: Mortality of MYT & (pseudo)faeces by MYT
6: Excretion by MYT & respiration by MYT
7: Dislodgement of MYT
8: PHYTO uptake by JAS
9: ZOO uptake by JAS
10: PELDET uptake by JAS
11: Mortality of JAS & faeces by JAS
12: Excretion by JAS & respiration by JAS
13: ZOO uptake by METR
14: Mortality of METR & faeces by METR
15: Excretion by METR & respiration by METR
16: PHYTO uptake by AQ
17: ZOO uptake by AG
18: PELDET uptake by AQ
19: Mortality of AQ & (pseudo) faeces by AQ
20: Excretion by AQ & respiration by AQ
21: Dislodgement of AQ
22: PHYTO uptake by ZOO
23: Mortality of ZOO & faeces by ZOO
24: Excretion by ZOO & respiration by ZOO
25: Mortality of PHYTO
26: N_2O emission by MYT
27: N_2O emission by AQ
28: Nitrification of NH4
29: Mineralisation of PELDET
30: Mineralisation of BOTDET

Figure 12 – Schematic model representation showing an offshore wind farm turbine foundation with vertical zonation of colonising fauna and the biogeochemical / biological processes between the different state variables Mytilus edulis *[MYT],* Jassa herdmani *[JAS],* Metridium senile *[METR], phytoplankton [PHYTO], zooplankton [ZOO], pelagic detritus [PELDET], bottom detritus [BOTDET],* M. edulis *aquaculture [AQ], emission of nitrous oxide [N2O], ammonium [NH4] and nitrate [NO3]. N_2O is exchanged at the air-water interface (double arrow). Diffusive transport and sinking of state variables are not shown.*

Aquaculture scenarios

The behaviour of the OWF ecosystem, and especially that of the three OWF AHS colonising species, was compared with and without the presence of a *M. edulis* longline aquaculture setup in multifunctional co-use with the offshore wind farm for each of the climate scenarios described above. The initial values of the state variable AQ were set to zero in the scenarios without

aquaculture, making it impossible for the AQ biomass to grow in response to system cues. Correspondingly, the total biomass of *M. edulis* in an aquaculture set-up (AQ) was modelled within and outside an OWF by setting the initial values of all three OWF AHS colonising species (MYT, JAS and METR) to zero in the latter. The total nitrogen in the system was identical in all scenarios (15 mmolN m^{-3}).

N_2O scenarios

The state variable N2O quantified the emission of N_2O by *M. edulis* and its associated shell biofilm on a OWF turbine scale. Emitted N_2O was only subjected to diffusive transport throughout the water column or exchanged at the water-air interface. The air-sea exchange was modelled using the temperature-dependent gas transfer velocity of N_2O and the difference in water vs. atmospheric equilibrium concentrations. Furthermore, the model was run with N_2O being produced by both MYT and AQ, or by MYT only to quantify the additional N_2O emission by a potential blue mussel aquaculture setup,.

4. SCIENTIFIC RESULTS AND RECOMMENDATIONS

4.1 Artificial Hard Substrate Garden

The AHSG mooring has proven to be of usable design that can provide the necessary epifauna for eg. experimental work in lab conditions where complete epifaunal communities or single species collections are needed, for in-situ follow-up of biofouling processes, study the interplay between biofouling and corrosion,…

The design is a simple, lightweight, and affordable construction that is sturdy enough to remain intact over a full year. Several of such moorings could be deployed in one single effort from a medium sized vessels and divers can easily collect the plates attached to a cage during one single dive window.

Retrieval of the moorings is in the current setup fully depending on divers who need to lift the anchor weight with lifting balloons. A vessel crew can then hoist anchor stone and the mooring on deck. Using divers to lift equipment is very depending on weather and tide and relatively time consuming. In theory acoustic releases could be used to lift the mooring to the surface. An acoustic release brings a smaller float with the rope to the surface from where the anchor stone can be hoisted on deck. Acoustic releases are unfortunately expensive equipment, and they might eventually fail in which case recovery by divers remains a necessity. For a prolonged deployment of the moorings in an AHSG the investment in acoustic releases would proof financially beneficial.

Using a marker buoy for fast location of the mooring has proven difficult. Both waves and currents cause loss of the surface float. The surface floats seem quite desirable and get stolen too. Using a surface float also clearly puts physical stress on the entire mooring and greatly jeopardizes loss of the entire mooring.

For the surface mooring a marker buoy is very much needed as a metal object at 3-5m below surface constitutes a serious navigational hazard. The PERSUADE project deployed the moorings in an offshore windmill farm and in known dedicated locations to the windmill farm operators. This excludes accidents to a large extend but even a larger surface marker buoy was lost during trials. Consequently, the last deployment of the mooring that held a cage in surface waters had the cage at 7m depth so that only very large vessels could collide with the subsurface float. An event that very likely would only damage the cage and go unnoticed to that vessel.

If one would need to have a durable surface marker buoy to indicate the location of the moorings in offshore areas and that survives storms, the whole construction would need to be re-designed drastically and be much heavier and heavy duty designed. Buoy laying vessels usually hoist first the buoy on deck and then haul in the chain and anchor. The PERSUADE design does not allow such a recovery. The cage will not hold the weight of the anchor stone and the chain used is unfit to lift it. Offshore buoys also need far more chain and a 5ton anchor stone. Such a mooring cannot be deployed with unequipped or small size vessels.

For research purposes we believe it is to be recommended to use only subsurface moorings and retrieve the small cages with divers or apply acoustic releases. A disadvantage might be that the mooring cannot be used for studies that need to span different years. After the last deployment of the project the three moorings could not be recovered before winter. Their recovery in spring will give insight in their condition and whether they are still afloat or not. Adding extra anodes to

prevent corrosion deterioration can help. Using heavier connectors and chackles might prolong lifetime at sea equally. Adding extra subsurface floats to keep a cage afloat for a longer period should also not pose serious issues.

The maintenance and repair costs of such low weight moorings is also less costly, and loss easily compensated for by constructing a new mooring. The total sum of one complete mooring is estimated to be around 2000€.

While the AHSG was mainly designed to serve PERSUADE purposes, and was only completed in year 2 of the project it has served other projects as well, including the Belspo-FaCE-IT project and the EDEN2000 project. The installation will be maintained after the lifetime of PERSUADE as a Belgian contribution to the European Marine Biological Resource Centre (EMBRC), and has a central position in the Belsp ESFRI-FED RBINS_EMBRC project (2022-2025).

Recommendation: the AHGS is a unique *in situ* test facility supporting fundamental ecological research on artificial hard substrate ecology and supporting applied research allowing a sustainable development of the Blue Economy. Given the increasing pressure to build human constructions at sea, we recommend to support the development of the AHSG as a long-lasting *in situ* test facility and aligning it with complementary services that are available in Belgium. We strongly suggest to make use of the EMBRC framework to embed the facility in a European context to increase its visibility and to allow Belgian partners to attract competitive funding and foster cooperation with high-level research institutes within Europe and beyond.

4.2 Effects of Climate Change on the ecophysiology of fouling species

Our experimental results confirmed our hypothesis that the ecophysiology of the important fouling species on OWF are significantly affected by ocean warming and acidification. Mortality of the blue mussel *M. edulis* and the amphipod *J. herdmani* was significantly increased in the CC treatments, and mortality in these treatments exceeded mortality in OW and OA treatments. This was not the case for the plumose anemone *M. senile* where significantly increased mortality was observed in the OW treamtents only (Fig. 14).

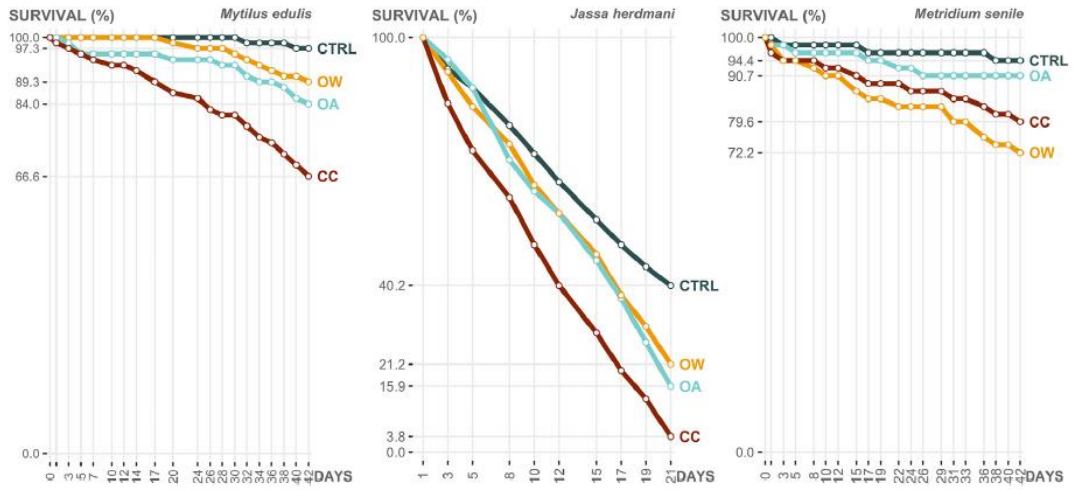

Figure 13. Proportional survival (%) of Mytilus edulis (left), Jassa herdmani (middle) and Metridium senile (right) throughout the six- and three-week experiments in four experimental treatments (CTRL: control, OA: ocean acidification, OW: ocean warming and CC: climate change). (From Voet et al. 2022)

We observed a significant additive effect of OW and OA on respiration of *M. edulis*, with highest respiration rates observed in CC. Similarly, respiration rates of J. *herdmani* were highest in the CC treatment, through a potentiating effect of the combination of both OA and CC. OA had no effect on the respiration rates of M. senile, where increased respiration was only observed in OW treatments (Fig. 15).

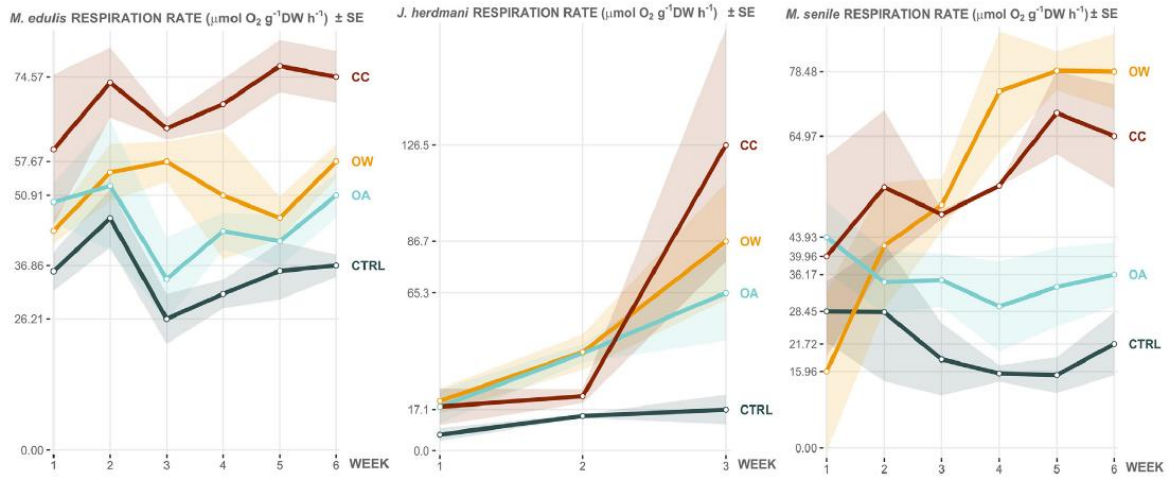

Figure 14. Mean respiration rate (µmolO_2 $g^{-}1$ DW h^{-1} ± SE shaded area) of Mytilus edulis *(left),* Jassa herdmani *(middle) and* Metridium senile *(right) throughout the six- and three-week experiments in four experimental treatments (CTRL: control, OA: ocean acidification, OW: ocean warming and CC: climate change). Note difference in scale.*

For both *M. edulis* and *J. herdmani*, OW and OA had an additive effect on clearance rates, which was again not the case for *M. senile*. Volumetric growth, measured for *M. edulis* and *J. herdmani* was negatively affected by CC through antagonistic effects of OW and CC.

Table 2– Data used for the calculation of estimated cumulative clearance potential of the artificial hard substrate fauna community inhabiting an OWF monopile foundation in the Belgian part of the North Sea (BPNS)

	VALUE	REFERENCE
Mean biomass (gDW ind^{-1})		
Mytilus edulis	0.785	This study
Jassa herdmani	0.002	This study
Metridium senile	1.651	This study
Total density (ind m^{-2})		
Mytilus edulis	1843	Mavraki et al (2020)
Jassa herdmani	24339	Mavraki et al (2020)
Metridium senile	480	Unpublished personal data
Total surface area (m^2)		
Mytilus edulis	192	Rumes et al (2013), as cited in Mavraki et al (2020)
Jassa herdmani	384	Rumes et al (2013), as cited in Mavraki et al (2020)
Metridium senile	220	Unpublished personal data
Mean diameter (m)		
Monopile foundation	7.25	Degraer et al (2016)

By integrating the experimental results with literature data (Table 2), we calculated the 'maximised cumulative clearance potential' of the fouling fauna on an OWF turbine in the BPNS, for the current and CC situation to estimate the total volume of seawater potentially cleared around a monopile foundation per day (m^3 d^{-1}). This revealed that the relatively small ecophysiological individual changes result in a important change in the effect on the surrounding water column, as the volume of cleared water increased from about 7.5 olympic swimming pools per day under current climate conditions to about 9 olympic swimming pools per day under future climate conditions. Through such a measurable effect on the water clearance, climate change and the increasing numbers of OWF installations in the North Sea could collectively affect the primary producer standing stock and zooplankton biomass in the vicinity of the OWFs (Boon et al., 2018; Mavraki et al. 2020c) and beyond (Slavik et al. 2019). This would further increase the organic matter flux to the sediment in- and outside the OWF (Ivanov et al. 2021) and could therefore alter local phytoplankton concentrations, which are very important for the OWF's ecological balance (Adhikary et al. 2021). In general, the predicted changes in OWF AHS community structure and functioning, in combination with their spill-over effect beyond the turbine foundation and the OWF perimeters, will impact the OWF's artificial reef effect and the interconnected (supporting) ecosystem services (Leadley et al. 2014, Causon & Gill 2018, De Borger et al. 2021).

Recommendation: Our results show that the impact of local activities to mitigate climate change will effectively interact with the effect of climate change and will collectively induce larger-scale changes in ecosystem functioning and associated ecosystem services. We recommend collecting data and results as presented here and using them for detailed ecosystem-based ecological modelling of integrated effects of multiple OWFs to support local energy policy and marine planning decisions in a globally changing climate.

4.3 Effects of Climate Change on N_2O production

Our results confirmed that a relatively large share (70%) of the N_2O production of mussels is related to the shell biofilm. This contribution remained constant, independent of warming or acidification treatments (Fig. 16).

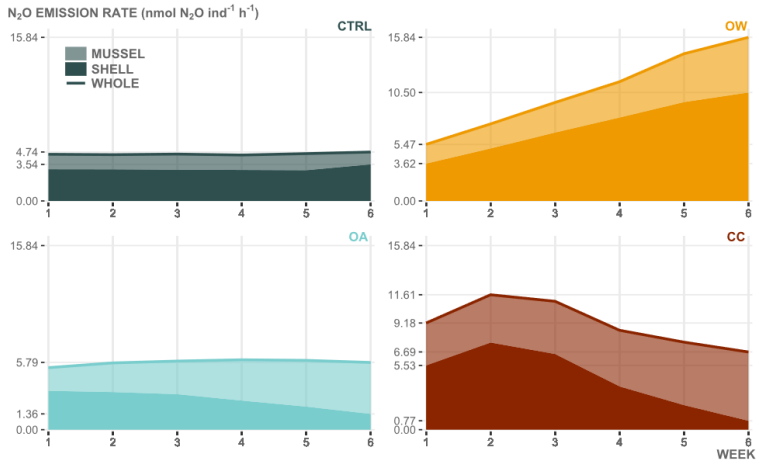

Figure 15 Estimated mean relative contribution of dissected Mytilus edulis *shells [SHELL] to whole animal [WHOLE] N_2O emission rates (nmol N_2O ind^{-1} h^{-1}) in four experimental treatments [CTRL: control, OA: ocean acidification, OW: ocean warming and CC: Relative contribution of* M. edulis *itself [MUSSEL] is calculated as WHOLE minus SHELL.*

All our experiments revealed an antagonistic effect of OW (increasing) and OA (decreasing) on N_2O production. Our inhibition experiments further suggested that he blue mussel *M. edulis* and its microbial shell biofilm produce N_2O through all three potential pathways, i.e. nitrification, denitrification and nitrifier denitrification, (using ammonium, nitrate and nitrite as a precursor, respectively), but denitrification of nitrite proved to be the main pathway. The relative importance of these pathways and the relative contribution of the shell biofilm to the blue mussel's total N_2O emission, as well as the biofilm thickness, coverage and most likely, composition, are affected by warming, acidification or the combination of both. Indeed, our detailed oxygen measurements above a mussel shell showed significant treatment differences (Fig. 17). At least 90% of the differences between the profiles in CTRL and the other experimental treatments could be attributed to the first 600μm above the shell surface. In OW, we observe a faster and stronger decrease in oxygen concentrations above the shell. In acidification treatments, the onset of the decrease in oxygenation is closer to the shell surface and the magnitude of decrease is lower

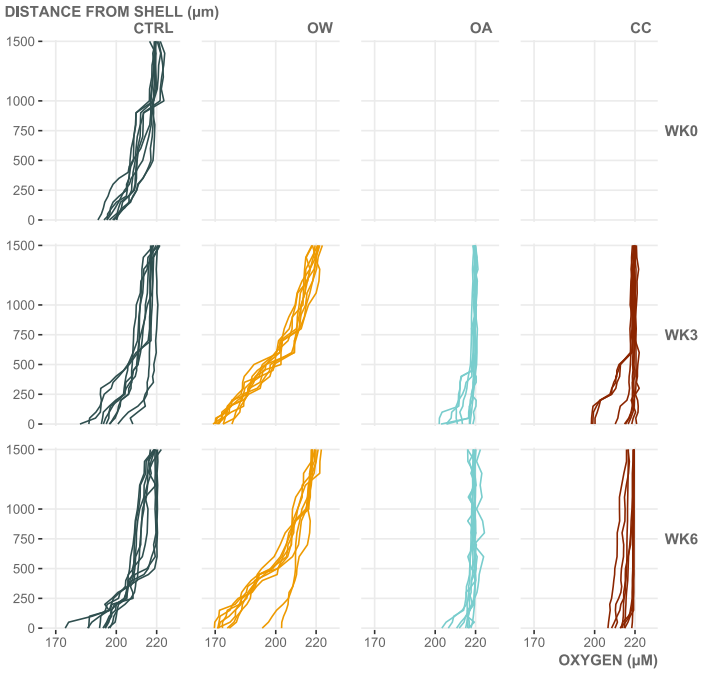

Figure 16 Vertical oxygen profiles of the microbial biofilm on Mytilus edulis *shells, 1500µm above the shell surface, before seawater manipulations started (WK0) and after three and six weeks of manipulations (WK3 and WK6, respectively) in each experimental treatment [CTRL: control, OA: ocean acidification, OW: ocean warming and CC: climate change]. Profiles were measured on three random locations per replicate* M. edulis *shell (n = 3) per time point and treatment.*

While the oxygen profiles revealed a change in the thickness of the biofilm, the molecular analysis did not reveal any significant impacts of the different laboratory-simulated climate change scenarios on the diversity of mussels' epi-microbiomes nor on the structure of microbial communities (fig. 18). Along the same lines, the aerobic respiration by the microbial biofilm was not significantly affected under stressful conditions. Conversely, the microbial community diversity and structure of the surrounding water were significantly affected by climate treatment (fig. 18).

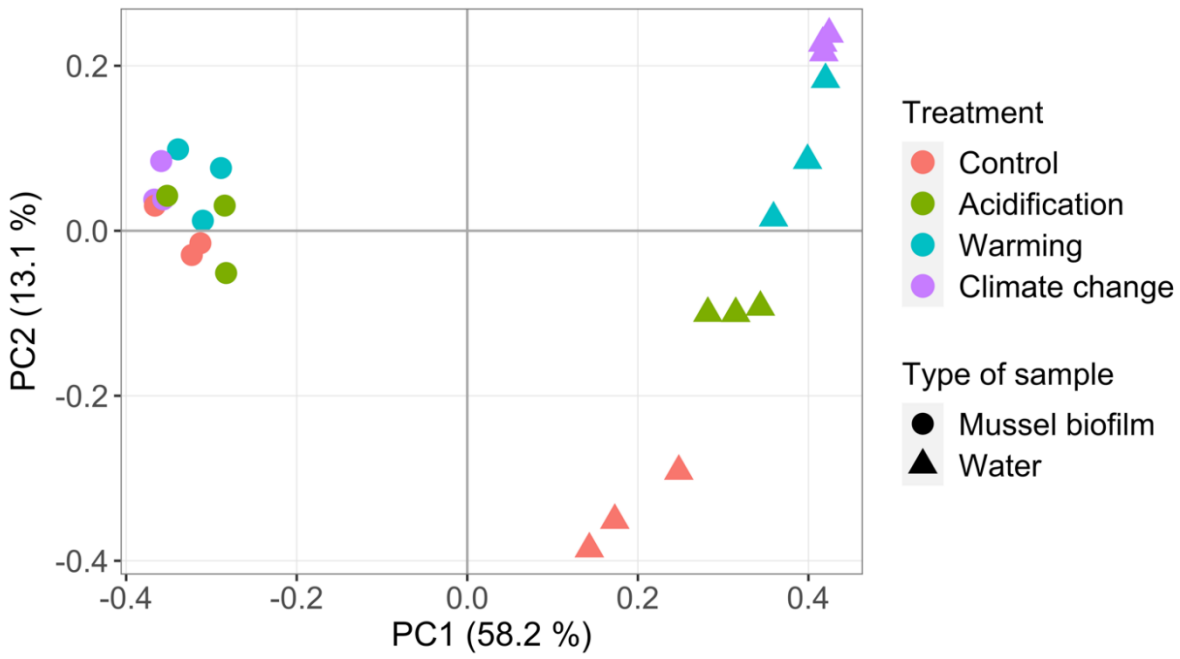

Figure 18. Microbial community structure. Principal coordinate analysis (PCoA) based on GUniFrac distance matrices evaluating the influence of simulated seawater acidification and/or warming on microbiomes ("Treatment" factor) of mussel biofilms and in the surrounding water column ("Type of sample" factor) after six weeks of incubation. While climate treatment substantially affected the water microbial communities, the mussel epimicrobiome remained remarkably stable throughout all treatments.

In contrast to the stable community structure of the mussel microbiomes, PICRUST analysis suggested clear changes in the functional roles of the mussel epimicrobiomes in relation to the N cycle in response to climate change. Moreover, these analyses suggest antagonistic functional effects of acidification and temperature rise (fig. 19). This appears in line with measured aerobic respiration and N_2O emission rates of microbial biofilms which decreased in acidified seawater but increased under warmer conditions.

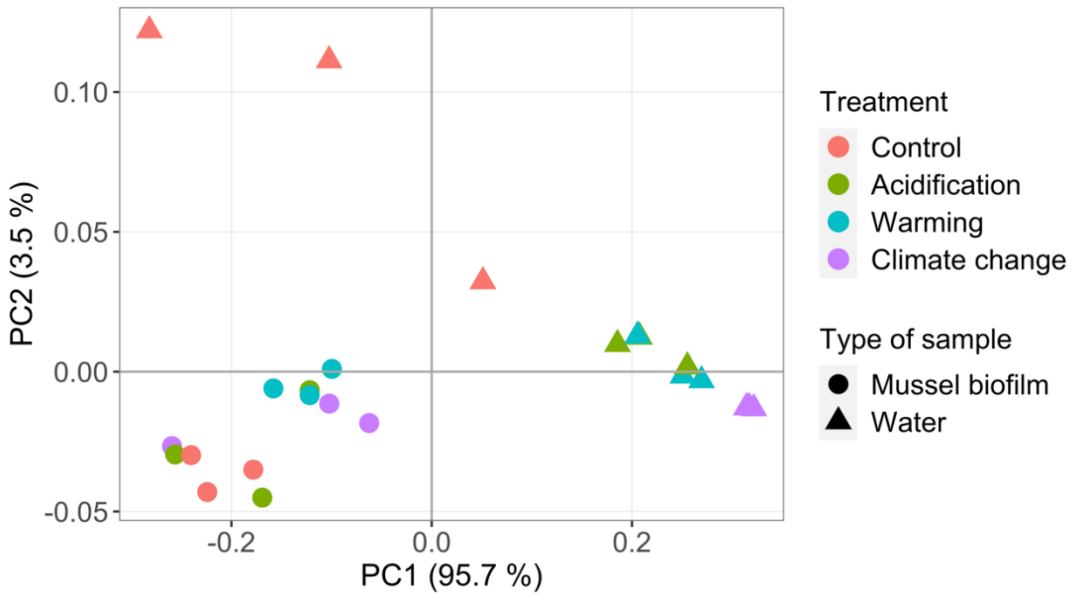

Figure 19. Predicted nitrogen metabolism pathways. Principal coordinate analyses (PCoA) ordination based on Bray-Curtis distance matrices evaluating the influence of experimental treatments ("Control", "Acidification", "Warming" and "Climate change") on the relative abundance of predicted metabolic pathways involved in the nitrogen cycle of microbial communities on the shell of mussels Mytilus edulis *and in the surrounding water column after six weeks of incubation. Note the separate functional clustering of epimicrobiome samples of the warming and CC treatments on one side, and of control and acidification on another side of the ordination plot.*

Recommendation: Our results reveal an additional N_2O production by mussels, where 70% of the N_2O production is provided by the shell biofilm. As N_2O is considered a potent greenhouse gas, we recommend to take this additional production of greenhouse gasses into account when estimating the effect of the introduction of offshore wind farms and offshore aquaculture activities. Further detailed research, linking N_2O production to shell size and to structural and functional changes in the shell microbiomes, and improved modelling (see below) are needed to upscale the local feedback links to climate change towards a regional level, where multiple OWFs are active and planned, and where aquaculture activities are on the horizon of the Blue Growth community.

4.4 Climate change effects on benthic biogeochemistry

Here, we only report the effects of the study organisms on oxygen penetration depth, SCOC, NHx effluxes, Nitrification and Denitrification after 6 weeks of exposure.

Both the clam *Abra alba* and the tube worm *Lanice conchilega* increased the oxygen penetration depth in the sediment, due to their sediment reworking and ventilation activities, respectively. While *Lanice conchilega* survival was unaffected by the multiple stressors imposed in the lab, *Abra alba* suffered from the increased temperature, with a 34% lower survival after 6 weeks of exposure to warmer conditions.

Under acidified conditions, *Lanice* had a stimulatory effect on SCOC, Nitrification and Denitrification with an increase of 37 %, 41 % and 25 % respectively (Figure 20). This can be explained by the increased ventilation activity of this tube-building polychaete under acidified conditions (Fig. 21).

In non-acidified conditions, *A. alba* significantly stimulates SCOC resulting in an increase of 35 % (Figure 20). This stimulatory effect disappears under acidified conditions. The effect of *A. alba* on nitrification and denitrification is affected by the combination of seawater pH and temperature: The rates are stimulated by the presence of *A. alba* in a climate change (CC) scenario, altering the negative interaction effect of seawater pH and organism presence (Figure 20). These patterns can be explained by the altered behaviour of *Abra alba*, since under climate change conditions, this bivalve appears to dwell closer to the surface.

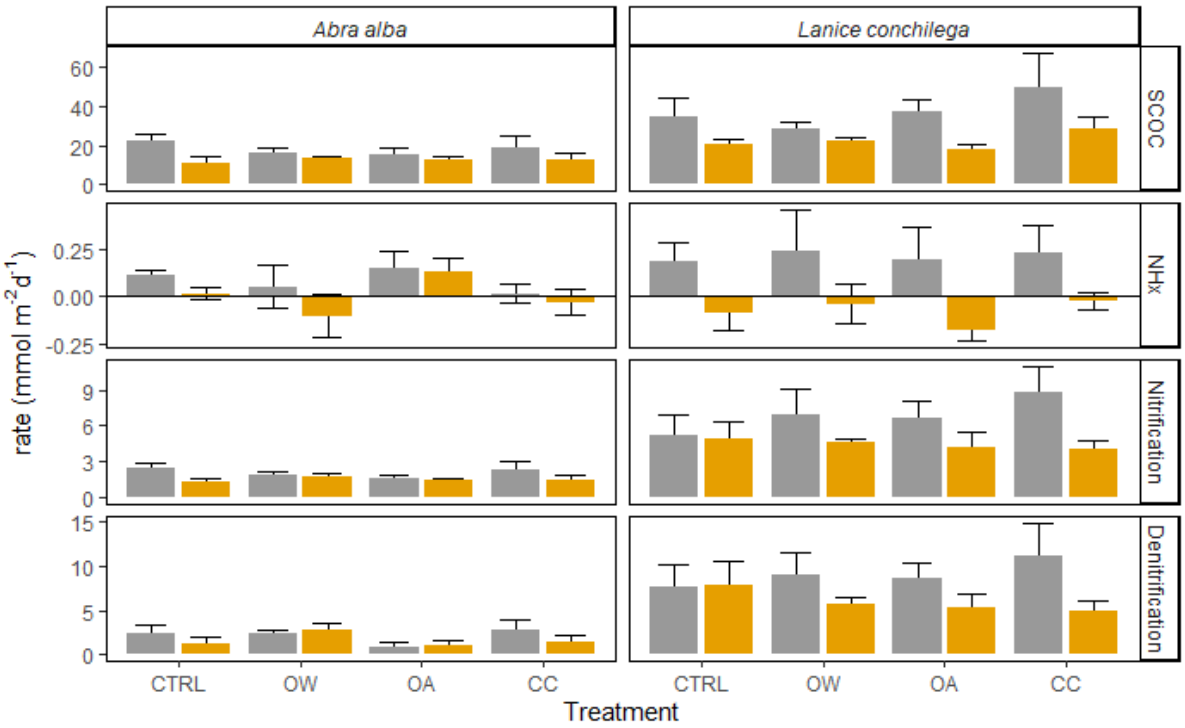

Figure 20: Effect of Abra alba *and* Lanice conchilega *presence (organism presence: grey bars; organism absence: yellow bars) on Sediment Community Oxygen Consumption (SCOC, in mmol O_2 m^{-2} d^{-1}), NHx effluxes, Nitrification and Denitrification (in mmol N m^{-2} d^{-1}) after 6 weeks of exposure to different temperature and pH scenarios: control (CTRL), Ocean warming (OW), Ocean acidification (OA) and the interaction between increased temperature and lowered pH (Climate Change, CC).*

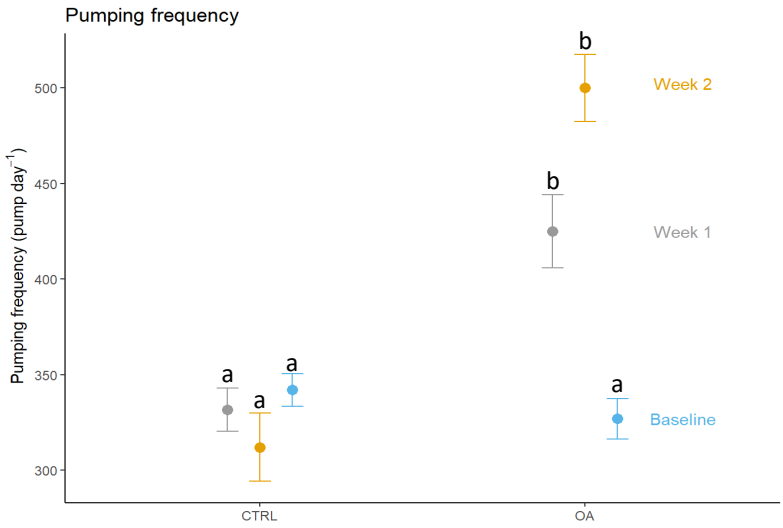

Figure 21. Pumping/burrow ventilation frequency of Lanice conchilega *after one and two weeks of incubation in control (CTRL) and acidified (OA) conditions. Data shown are means and standard errors (± SE) of four replicates per treatment. Letters represent compact letter display of significant differences between treatments.*

Conclusion: Sediment-inhabiting organisms in burrows or tubes might ventilate their environment more frequently in future climate scenario's (particularly ocean acidification). This flushing of the seabed stimulates nutrient cycling, and at moderate densities of tube worms, also increases the nitrogen filtering capacity of the sediment (denitrification). Bivalves on the other hand, suffer from future climate scenarios (warming and acidification): they move closer to the sediment surface and after prolonged exposure experience increased mortality rates. The stimulatory effect of bivalves on sediment oxygenation, nutrient cycling and the nitrogen filtering capacity of the sediment (denitrification) therefore decreases under future climate scenarios.

Recommendation: Take into account that stimulatory effects of benthic fauna on marine ecosystem services such as nutrient cycling might change under future climate scenarios, and that the effects of long-term exposure to climate change on bioturbators and bio-irrigators are currently unknown. Climate change is only one of the cumulative pressures on the benthic ecosystem. Our results suggest that to maintain nutrient cycling by benthic communities, it would be recommendable to increase the level of protection of benthic communities from other stressors such as anthropogenic impacts on the seabed.

4.5 Effects of Climate Change and mariculture on food-web flows

In this study, the carbon assimilation by the typical OWF colonising fauna and associated sediment community was experimentally quantified under current and future climate conditions, including a 'multifunctional co-use' scenario with blue mussel (*M. edulis*) aquaculture activities within the OWF area. The results confirmed our hypotheses: (1) biomass-specific and total carbon assimilation differed significantly between OWF species across different trophic levels, (2) climate change conditions significantly altered biomass-specific carbon assimilation of AHS colonising fauna and (3) the presence of *M. edulis* aquaculture significantly reduced biomass-specific carbon assimilation of the key species in a closed mesocosm OWF AHS system. Here, we will focus the results on the effects of climate change and *M. edulis* aquaculture on the carbon assimilation by the turbine-associated food web.

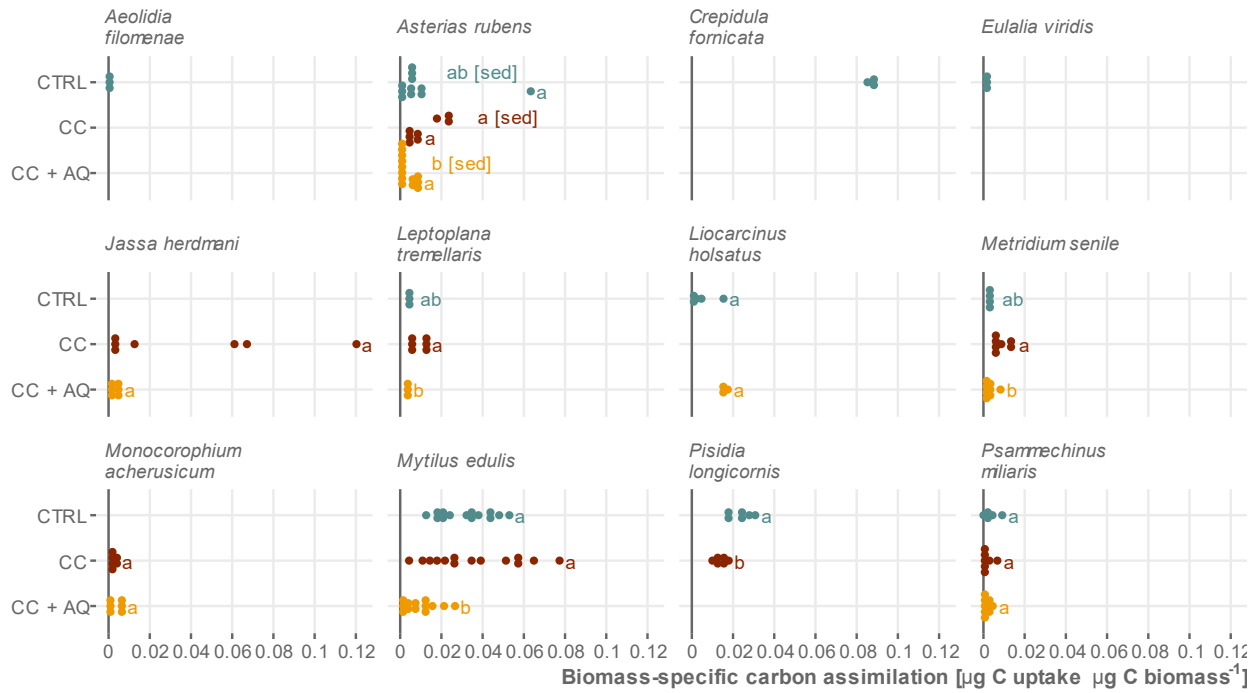

Figure 22 – Biomass-specific carbon assimilation [µgC µgC$^{-1}_{biomass}$] per species and per mesocosm. Letters represent compact letter display of significant differences between mesocosms within each species (Kruskal-Wallis Rank Sum test): mesocosms sharing a letter do not differ significantly after Bonferroni correction.

In the CTRL mesocosm, the biomass-specific carbon assimilation of the limpet *C. fornicata* and blue mussel *M. edulis*, both feeding directly on the ^{13}C labelled algae, was significantly higher than all other species present, including both direct and indirect consumers (Figure 22), as was observed before (Mavraki et al. 2020c). In the Climate Change (CC) mesocosm, more species assimilated the algal carbon compared to the control. Here, the amphipod *J. herdmani* and long-clawed porcelain crab *P. longicornis* had the highest biomass-specific carbon assimilation in the CC mesocosm alongside *M. edulis*. Both *J. herdmani* and *P. longicornis* are known to opportunistically feed on suspended organic material (phyto- and zooplankton, as well as detritus) or on *M. edulis* pseudofaeces, respectively ((Dixon & Moore 1997, Tenore and González 1975), meaning such a combined feeding method proved successful in the CC environment. (Tenore & Gonzalez 1976, Dixon & Moore 1997). This combined feeding method proved successful in the

CC environment. The combined direct and indirect uptake of the labelled algae, as well as the typically increased feeding rates of 'direct consumers' such as *M. edulis* in a warmer environment, are likely explanations for the observed structural shift in terms of topmost species' biomass-specific carbon assimilation within this future climate scenario (Jørgensen et al. 1990, Voet et al. 2022). In addition, well-fed *M. edulis* produces (pseudo)faeces with undigested algal cells (Riisgård et al. 2011), which could further explain the relatively high biomass-specific carbon assimilation by 'indirect consumers' such as *P. longicornis* in the CC mesocosm, compared to the CTRL environment .

In the future climate aquaculture scenario (CC+AQ), the highest biomass-specific carbon assimilation was measured in *M. edulis*, *A. rubens* and the flying crab *L. holsatus*. The latter are active predatory species with a preference for bivalves (i.a. *M. edulis*) or a preference for crustaceans and bivalves (especially *M. edulis*), respectively (Choy 1986, De Mesel et al. 2013). In the CC+AQ mesocosm, these predators had ample food sources available. This lead to another structural shift in top consumers, from direct or combined (in)direct consumers of labelled algae to also higher trophic-level predatory species. Overall, however, the average carbon assimilation was lower in CC+AQ compared to the other mesocosms, most likely due to an increased interspecific competition for a limited food source. Given the mesocosms in this study were closed ecosystems and the added ^{13}C labelled algae reflected the natural mean *in situ* phytoplankton biomass (Baretta-Bekker et al. 2009) at the start of the experiment, a certain degree of interspecific competition for this limited food source was to be expected.

It is therefore expected that the introduction of a substantial aquaculture standing stock into an OWF will have its repercussions on the local ecosystem. In an ecological modelling study on OWFs in the BPNS, both biomass and phenology of important food web components (i.a. phyto- and zooplankton) and dominant OWF AHS colonising species (i.e. *M. edulis, J. herdmani* and *M. senile*) were affected by the introduction of *M. edulis* aquaculture (Voet et al. in prep.).

Several measures were taken to create mesocosms that accurately reflect the OWF natural species composition (De Mesel et al. 2013, Kerckhof et al. 2019, Mavraki et al. 2020c). Nevertheless, differences in species composition and abundance between mesocosms were observed at the start of the experiment. These differences resulted from the random distribution of the AHS panels and sediment containers across the environmental treatments, as these were not quantified or altered before incubation in the mesocosms. Furthermore, the relative distribution of species biomass in the mesocosms was not necessarily representative of that found in OWF ecosystems. The tube-building amphipods *J. herdmani* and *M. ascherusicum* were heavily underrepresented in the mesocosms compared to natural situations (Mavraki et al. 2020b), likely due to a high mortality rate in relatively long-term experimental conditions (Beermann & Purz 2013). Additionally, a higher mortality rate in the climate change environment was expected, as amphipods are sensitive to changes in seawater temperature and/or pH (Poulin & Mouritsen 2006, Jakob et al. 2016, Voet et al. 2022). The relative abundance of the plumose anemone *M. senile*, one of the dominant hard substrate colonising species in the North Sea (De Backer et al. 2020, Degraer et al. 2020a), together with that of the common starfish *A. rubens* and the green sea urchin *P. miliaris*, both among the most abundant mobile predators found on the OWF foundations, was unintentionally low compared to actual in situ conditions (De Mesel et al. 2013, De Backer et al. 2020). Finally, a fully crossed experimental set-up between climate change and aquaculture scenarios was logistically not feasible, though its added value in unravelling and

uncoupling the effects of both stressors on the OWF colonising community is apparent and acknowledged.

Nonetheless, the experimental work performed in this study was innovative in its use of pulse-chase techniques on an ecosystem-wide scale in current and future climate scenarios. The use of large, environmentally manipulated mesocosms allowed us to incorporate various species interactions (e.g. predation and competition) and capture direct and indirect effects (e.g. on filter- and detritus feeders, respectively), therefore proving to be highly relevant on an ecological scale.

The presence of an aquaculture set-up in OWF settings that are already heavily populated by filter feeders, substantially increases the filtration capacity towards the top of the water column and the production carrying capacity is only sustainable if nutrient or organic matter extraction by the mussels is balanced with ecosystem food replenishment. Therefore, the introduction of bivalve mariculture will undoubtedly affect, and in turn be affected by, the local ecosystem (Cranford 2019; Costello et al. 2020). Moreover, such a combined multi-use could even alter or exacerbate potential climate change effects on the OWF AHS ecosystem functioning. Indeed, this study identified varied functional and structural changes when exposing the OWF ecosystem to future climate conditions or future climate conditions with the additional presence of blue mussel aquaculture. Manipulated climate change conditions suggested a shift towards the inclusion of 'indirect' consumers in addition to the 'direct' consumers already prominent in the current climate and when aquaculture activities were also present, another shift in top consumers with a propensity towards higher trophic-level predatory species was observed.

Recommendation: Studies looking at the structure and functioning of an OWF ecosystem in different parallel climate and multi-use scenarios, are needed to anticipate the critical juncture where the various technical and legislative complexities of implementing offshore aquaculture in multifunctional co-use with offshore renewable energy might be overshadowed by the global ecological and economic impacts of climate change. Furthermore, to find a balance between offshore wind energy development, seafood production, nature conservation and future climate stressors, the knowledge provided by similar topical studies and pilot projects, as well as the patronage of blue economy through potential incentives for commercial multifunctional co-use, will need to be incorporated in governmental marine spatial planning processes.

We advise simulating effects of climate change and multiuse in large, environmentally manipulated mesocosms, as it allows incorporating many species interactions (e.g. predation and competition) and capturing direct and indirect effects (e.g. on filter- and detritus feeders, respectively), therefore proving to be highly relevant on an ecological scale.

4.6 Ecological modelling

PERSUADE resulted in first version of an ecological model that made use of experimentally derived relevant data to assess the combined effects of local activities (OWF without/in combination with aquaculture activities) and global change. Currently, the model is under further development, and we restrict ourselves to reporting a proof of concept. We aim to reveal the relevance of detailed ecophysiological and biogeochemical research as it provides the actual data needed for an accurate assessment of the consequences of human activities at sea.

Our climate simulation runs showed adverse effects of climate change on the three dominant fouling species. *M. edulis* (seems to benefit from climate change (probably a consequence of higher food availability), which is to certain extent mirrored in the patterns for *J. herdmani* (Fig. 23).

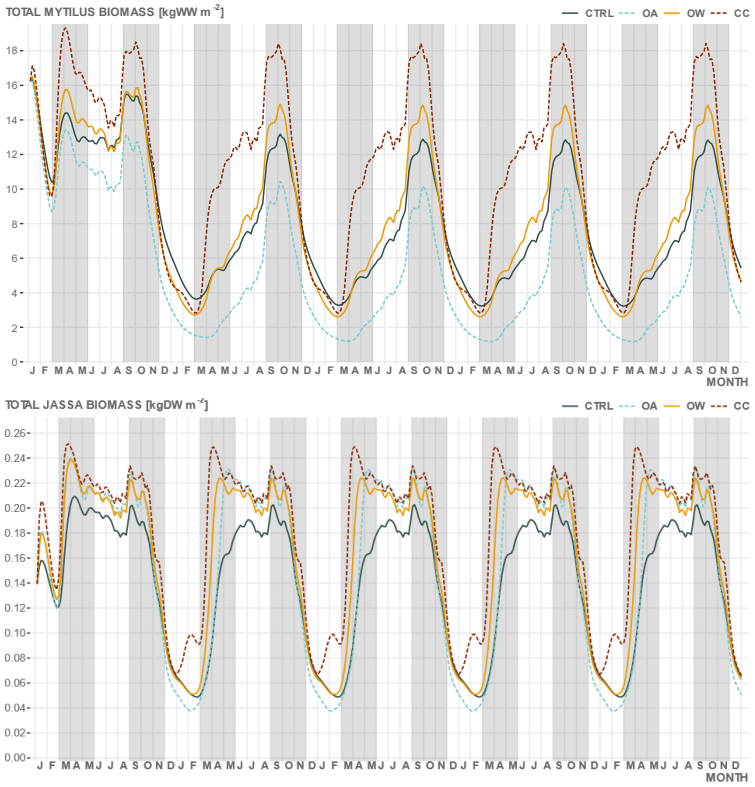

Figure 23. Total M. edulis *biomass [top; kgWW m^{-2}] and* J. herdmani *biomass [bottom; kgDW m^{-2}] in four climate scenarios: control [CTRL], ocean acidification [OA], ocean warming [OW] and climate change [CC].*

Adverse patterns were observed for *M. senile* (Fig. 24) where climate change clearly triggered a decrease in biomass.

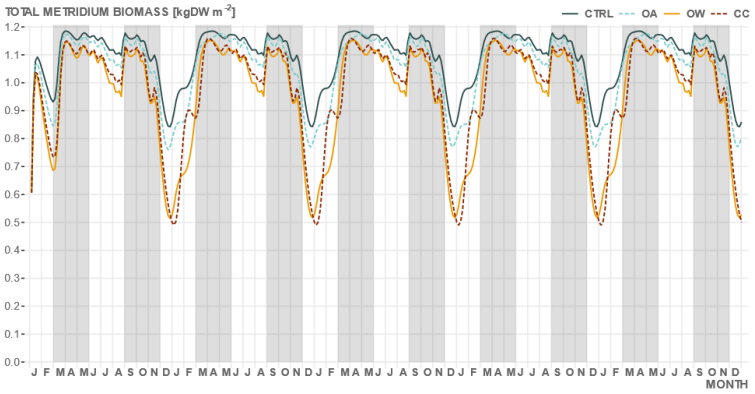

Figure 24 Total M. senile *biomass [kgWW m^{-2}] in four climate scenarios: control [CTRL], ocean acidification [OA], ocean warming [OW] and climate change [CC].*

Aquaculture activities in the area would yield about 6 kg wet weight of mussels per m² in the current conditions, and are projected to increase in future climate settings (Fig. 25).

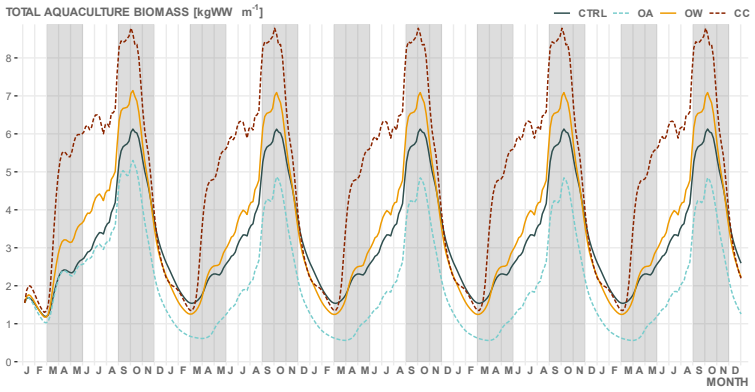

Figure25 Total M. edulis *aquaculture biomass [kgWW m^{-2}] in four climate scenarios: control [CTRL], ocean acidification [OA], ocean warming [OW] and climate change [CC].*

On the other hand, the presence of aquaculture activities results in a lower biomass of *M. edulis* on the turbines, suggesting a competition for food within the OWF area (Fig. 26).

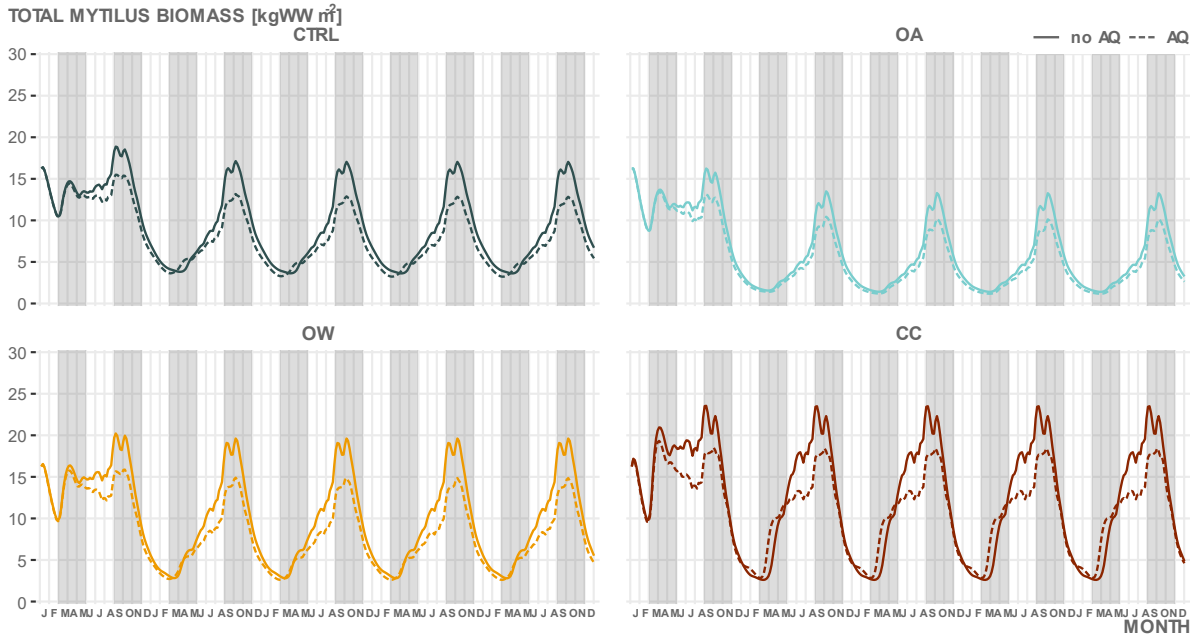

Figure 26. Total M. edulis *biomass [kgWW m^{-2}] present on the OWF turbine with or without the additional presence of* M. edulis *aquaculture [AQ] within the OWF in four climate scenarios: control [CTRL], ocean acidification [OA], ocean warming [OW] and climate change*

Aquaculture activities within the OWF increase the N_2O emissions to the atmosphere in all climate scenarios, but especially in the scenarios where ocean warming is present (OW and CC, Fig. 27).

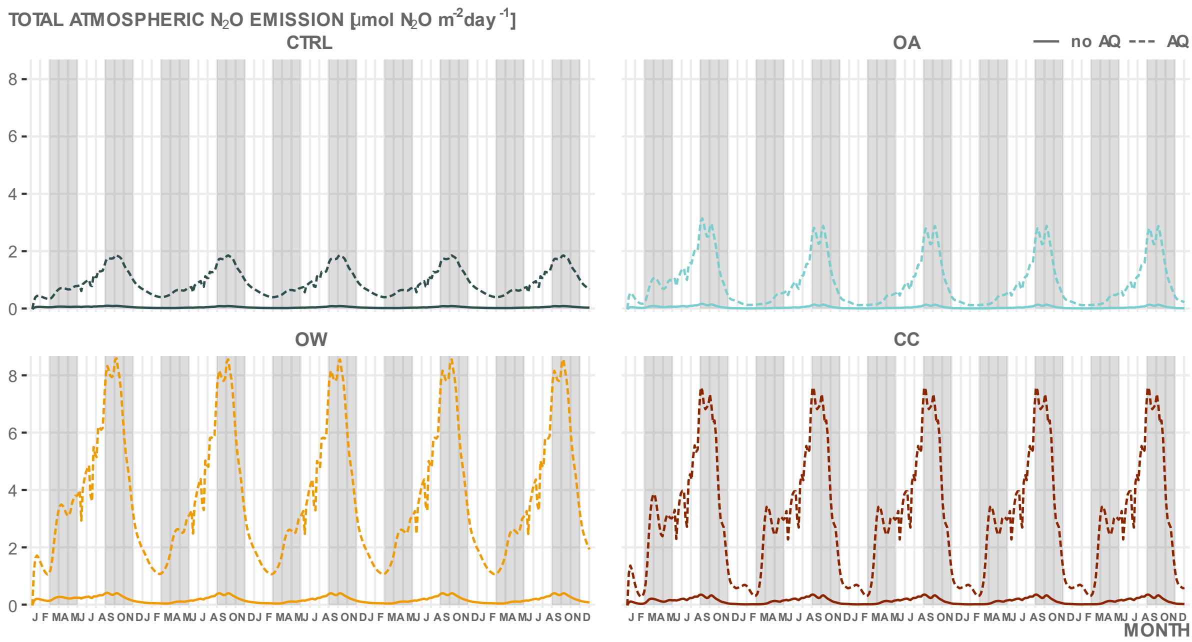

Figure 27. Total atmospheric N_2O emission [µmol N_2O m^{-2} day^{-1}] with or without the additional presence of M. edulis aquaculture [AQ] within the OWF in four climate scenarios: control [CTRL], ocean acidification [OA], ocean warming [OW] and climate change [CC].

Recommendation: predictive models, based on relevant data derived from targeted experiments, can be of great help to guide future management decisions with respect to multiple use of OWF areas. We recommend to further invest in the experimental research underlying the predictive models and the development of the models as well. The models should be generic, and ready to inform the planning of commercial activities and at the same time reflect important consequences of these activities. Furthermore, coupling such ecological models with models used by environmental economists would greatly increase the capacity of society to move towards objective trade-off analyses for alternative management scenarios.

4.7 Added value of PERSUADE research

PERSUADE has resulted in an important legacy with respect to developed infrastructure. The Artificial Hard Substrate Garden was developed for PERSUADE experimental purposes, and is the only *in situ* test installation, spanning the entire water column, in offshore highly dynamic condition. It is clear that the AHSG served the bulk of the PERSUADE experiments reported upon here, but it should be noted that it also was used by the FaCE-It and Eden2000 projects, despite its short existence. The AHSG is further mentioned in several research proposals and is at the heart of the recently started ESFRI-FED RBINS_EMBRC project (2022-2025) that will embed the AHSG in the service portfolio of the Belgian node of the European Marine Biological Resource Centre and open it up to international users via EMBRC-ERIC. Additionally, PERSUADE further modified the experimental tanks available at VLIZ that are now ready to host large scale experiments on climate change in controlled conditions. The strength here is the modularity of the experimental set up, allowing for a flexible use of the facilities. Part of the PERSUADE

adaptations have been used to construct a nursery for seaweed cultivation purposes in an attempt to stimulate seaweed aquaculture as important component of Belgian Blue Growth initiatives.

While the detailed scientific achievements are being published now, and therefore have scientific value on their own, we draw the attention to the progress that was made through the ecological modelling work, where we managed to run multi-use scenarios (OWF and aquaculture) in current and future climate settings, providing insights in both aquaculture yields and functional feedback links towards the environment. To our knowledge, such model is highly original and it is therefore an important part of planned work to investigate effects of co-located activities or societal trade-offs of different management scenarios.

Last but not least, PERSUADE built a bridge between fundamental and applied science, and academia and industry. In cooperation with the Blue Cluster EDULIS project and commercial partners, PERSUADE organised a workshop on anchoring techniques. This stemmed from the PERSUADE initiative to build an AHSG that needs to withstand the rather dynamic circumstances in the offshore part of the BPNS, and the desire to start bivalve and seaweed aquaculture activities in offshore OWFS.

5. DISSEMINATION AND VALORISATION

PERSUADE research was disseminated through a variety of channels, including the PERSUADE ResearchGate page (https://www.researchgate.net/project/PERSUADE-ExPERimental-approaches-towards-Future-Sustainable-Use-of-North-Sea-Artificial-HarD-SubstratEs), contributions to scientific events and participation to Ocean Literacy events.

The Research Gate page resulted in 591 reads, a number that is expected to increase in the future, as we will update the Research Gate page with PERSUADE papers that are currently being submitted. As such, the Research Gate page will act as a repository of all scientific output of the project.

We further communicated with a scientific audience through participation to a number of national and international conferences and a published paper. Due to the outbreak of the corona pandemic, the finalisation of 2 PERSUADE PhDs is delayed, but ongoing. Currently, at least 4 manuscripts are submitted or close to being submitted and more are expected.

PERSUADE knowledge and expertise was further widely used in an international context, notably in the United States where PERSUADE results and knowledge was used in the 2020 State of the Science Workshop on Wildlife and Offshore Wind Energy 2020: Cumulative Impacts, organised by the New York State Energy Research and Development Authority (NYSERDA, see https://www.nyetwg.com/2020-workshop). Along the same line, PERSUADE scientists and science were involved in the US Offshore Wind Synthesis of Environmental Effects Research, lead by the US Department of Energy Office of Energy Efficiency & Renewable Energy Wind Energy Technologies Office, the Pacific Northwest National Laboratory (PNNL) and National Renewable Energy Laboratory (NREL) (https://tethys.pnnl.gov/us-offshore-wind-synthesis-environmental-effects-research-seer).

Closer by home, PERSUADE science is used in the EDEN2000 project, investigating possible effects of the installation of future OWF in the Natura2000 zone of 'De Vlaamse Banken", and informal (and confidential) interactions with the Cabinet of the Minister of the North Sea and the Federal Public Service Health, Food Chain Safety and Environment.

PERSUADE interacted with commercial parties by co-organising a workshop on anchoring techniques for offshore installations, and was mentioned on the website of the Blue Cluster (https://www.blauwecluster.be/nieuws/proeftuin-voor-substraten-op-zee).

Communication with the public at large was achieved through participation of PERSUADE Scientists at several citizen science initiatives (ZeeUitzicht 2019, 2020), PaStory and the 'Westvlaamse Natuurstudiedag 2022'.

6. PUBLICATIONS

Oral Presentations:

Braeckman U, Lefaible N, Moens T, Vanaverbeke J, Degraer S. Functioning of the benthic ecosystem in OWFs: food webs and biogeochemical cycling. The 52nd International Liège colloquium on ocean dynamics. 17-21 May 2021, online conference

Degraer S et al, "From observing structural effects to understanding functional effects of offshore wind energy development", State of New York "State of the Science Workshop on Wildlife and Offshore Wind Energy". Woodbury, NY (USA), 13-15 November 2018. Invited speaker.

Degraer S. IBAMA Complexos eólicos offshore: Workshop internaçional avaliação de impactos ambientais. Brasilia (BR), 02-03 July 2019. Invited speaker.

Degraer S. Thünen symposium "Offshore wind farms and marine resources, Bremerhaven (DE) 12-13 November 2019. Invited keynote speaker.

Degraer S. North Sea Regional Advisory Committee, Environmental Committee meeting "Offshore wind farm environmental impacts with special attention to fish", Brussels (BE), 11 February 2020. Invited speaker.

Degraer S. Belgian Offshore Platform statutory meeting "Offshore wind farm environmental impacts: Overviewing 10 years of monitoring and research", Brussels (BE), 20 February 2020. Invited speaker.

Degraer S. WOZEP workshop "Offshore wind farm environmental impacts: Towards answering the "so what" question…", Den Haag (NL), 24 February 2020. Invited speaker

Vanaverbeke J, Braeckman U, De Borger E, Mavraki N, Toussaint E, Voet H, Van Colen C; Degraer S. Interactions between biological and physical effects modify local biogeochemical cycling processes in offshore wind farms. EMBS 53, Oostende, Belgium 17 – 21 September 2018

Vanaverbeke J, Dannheim J, Birchenough S, Capet A, Causon P, Coolen J, Degraer S, Hooper T, Janas U, Krone R, Lindeboom H, Mavraki N, O'Beirn F, Soetaert K, Toussaint E, van der Knaap I, Van Hoey G, Voet H, Wrede A. Ecosystem changes associates with offshore wind farms: bridging the gap between biogeochemical effects and its repercussions for ecosystem functioning and services. EuroMarine General Assembly, Cadiz, Oostende 30-31, January 2019

Vanaverbeke J, Dannheim J, Birchenough S, Capet A, Causon P, Coolen J, Degraer S, Hooper T, Janas U, Krone R, Lindeboom H, Mavraki N, O'Beirn F, Soetaert K, Toussaint E, van der Knaap I, Van Hoey G, Voet H, Wrede A. Towards a quantification of the effect of offshore wind farms on the provisioning of marine ecosystem services. Symposium 'Marine resources and offshore wind farms'. Bremerhaven, Germany, 12-13 November 2019.

Vanaverbeke J, Braeckman U, De Borger E, Mavraki N, Toussaine E, Voet H, Van Colen C, Degraer S. Towards Estimating the Biogeochemical Footprint of an Offshore Windfarm. ASLO Ocean Science Meeting, San Diego, USA, 16-21 February 2020

Voet H, Van Colen C and Vanaverbeke J (2019). *Ecophysiology and survival of the Blue mussel (Mytilus edulis) as offshore wind farm fouling and aquaculture key species, is adversely affected by a changing marine climate*. In Mees J et al. (Ed.) Book of abstracts – VLIZ Marine Science Day. Bredene, Belgium, 13 March 2019.

Voet H, Van Colen C, Vanaverbeke J. Marine climate change disrupts ecophysiology of the offshore wind farm fouling and aquaculture key species Blue mussel (*Mytilus edulis*). Conference on Wind Energy and Wildlife Impacts. Stirling UK. 27 – 30 August 2019

Voet H, Van Colen C, Vanaverbeke J. Investigating the combined effects of climate change on offshore wind farm fouling fauna: disrupted ecophysiology of Blue mussel (Mytilus edulis). The 52nd International Liège colloquium on ocean dynamics. 17-21 May 2021, online conference

Vlaminck E & Voet H, Cattrijsse A, Degraer S, Moens T, Soetaert K, Van Colen C and Vanaverbeke J (2019). *Experimental approach towards understanding food web interactions in an offshore wind farm environment under different climate scenarios*. Oral presentation at Conference on Wind Energy and Wildlife Impacts 2019, 27-30 August 2019, Stirling (UK).

Vlaminck E, Van Colen C, Vanaverbeke J, Moens T. Burrowowing macrofauna modifies climate change effects on sediment metabolism. The 52nd International Liège colloquium on ocean dynamics. 17-21 May 2021, online conference

Poster Presentations

De Meester N, Voet H, Vlaeminck E, Rigaux A, Degraer S, Vanaverbeke J, Moens T. Effect of climate change on the microbiome of the blue mussel. VLIZ Science Day, Bredene 13 March 2019

Voet H, Van Colen C, Van den Bulcke L, Vanaverbeke J (2018). *Investigating the combined effects of climate change on ecophysiological response of offshore wind farm fouling fauna*. VLIZ Marine Scientist Day, Bredene, Belgium 21 March 2018. VLIZ Special Publication, 80: pp. 127

Voet H, Van Colen C, Van den Bulcke L, Vanaverbeke J (2018*). Investigating the combined effects of climate change on ecophysiological response of offshore wind farm fouling fauna*. 53rd European Marine Biology Symposium. Oostende, Belgium, 17-21 September 2018. VLIZ Special Publication, 82: pp. 66

Voet H, Van Colen C and Vanaverbeke J (2019). *Marine climate change disrupts ecophysiology of the offshore wind farm fouling and aquaculture key species Blue mussel (Mytilus edulis).* Poster presentation at Conference on Wind Energy and Wildlife Impacts 2019, 27-30 August 2019, Stirling (UK).

Vlaminck E, Vanaverbeke J, Soeataert K, Moens T and Van Colen C (2018). Macrobenthos-mediated nutrient cycling in offshore wind farm environments under future ocean climate settings. VlIZ Marine Science Day, Bredene, Belgium 21 March 2018. VLIZ Special Publication, 81: pp.126

Vlaminck E, Vanaverbeke J, Soeataert K, Moens T and Van Colen C (2018). Macrobenthos-mediated nutrient cycling in offshore wind farm environments under future ocean climate settings. 53rd European Marine Biology Symposium. Oostende, Belgium, 17-21 September 2018. VLIZ Special Publication, 82: pp. 65

Vlaminck E & Voet H, Vanaverbeke J, Soeataert K, Moens T and Van Colen C (2019). Experimental approach towards the understanding of food web interactions in an offshore wind farm environment under different climate and aquaculture scenarios. VLIZ Marince Science Day, Bredene, Belgium 13 March 2019.

Papers/Manuscripts (published or submitted)

Vlaminck, E., Cepeda, E., Moens, T. & Van Colen, C. (submitted a) Ocean acidification modifies behavior of shelf seabed macrofauna: a laboratory study on two ecosystem engineers, *Abra alba* and *Lanice conchilega*. Submitted to Animal Behaviour

Vlaminck, E., T. Moens, J. Vanaverbeke & C. Van Colen (submitted b) Physiological response to ocean acidification reduces fitness of a benthic bio-engineer, the bivalve *Abra alba*. Submitted to Marine Environmental Research

Voet HEE, Van Colen C, Vanaverbeke J (2022) Climate change effects on the ecophysiology and ecological functioning of an offshore wind farm artificial hard substrate community. Science of The Total Environment 810:152194.

7. ACKNOWLEDGEMENTS

The PERSUADE consortium acknowledges Belspo for funding this project, and especially Koen Lefever for the excellent guidance and interest. Our research largely benefitted from scientific equipment made available by EMBRC-Belgium (funded through FWO project GOH3817N), and the scientific diving teams of VLIZ and RBINS. We are very grateful to the ILVO aquaculture project Value@Sea and the WinMon.BE project for providing organisms for our experiment. Our work was further supported by by data and infrastructure provided by VLIZ as part of the Flemish contribution to LifeWatch and by logistic support from the Research Vessel Simon Stevin.

We also would like to thank the members of the follow-up committee (prof dr. Frank Maes - UGent, dr. Nancy Nevejan – UGent, dr. Daan Delbaere – ILVO, dr. Saskia Van Gaver – FOD Leefmlieu, Dienst Marien Milieu, dr. Sarah van den Eede – WWF Belgium, Lien Loosvelt – De Blauwe Cluster, Willy Versluys – BREVISCO en Annemie Vermeylen – Belgian Offshore Platform) for their enthusiastic and constructive comments during the project.

LITERATURE

Adhikary S, Chaturvedi SK, Banerjee S, Basu S (2021) Dependence of Physiochemical Features on Marine Chlorophyll Analysis with Learning Techniques. In: *Advances in Environment Engineering and Management*. Springer Proceedings in Earth and Environmental Sciences, Siddiqui NA, Bahukhandi KD, Tauseef SM, Koranga N (eds) Springer International Publishing, Cham, p 361–373

Anderson MJ (2001) A new method for non-parametric multivariate analysis of variance. Austral Ecol 26:32–46.

Anderson MJ (2006) Distance-based tests for homogeneity of multivariate dispersions. Biometrics 62:245–253.

Anderson MJ, Gorley RN and Clarke KR (2008) PERMANOVA+ for PRIMER: guide to software and statistical methods. Primer-E Plymouth

Anderson MJ (2017) Permutational Multivariate Analysis of Variance (PERMANOVA). Wiley StatsRef Stat Ref Online:1–15.

Baretta-Bekker H, Bot P, Prins T, Zevenboom W. Report on the second application of the OSPAR Comprehensive Procedure to the Dutch marine waters. Rijkswaterstaat, The Hague. 2008 May.

Barton K (2020). MuMIn: Multi-Model Inference. R package version 1.43.17. <https://CRAN.R-project.org/package=MuMIn>Bates D, Mächler M, Bolker B, Walker S (2015) Fitting Linear Mixed-Effects Models Using lme4. J Stat Softw 67:1–48.

Bates D, Mächler M, Bolker BM, Walker SC (2014) Fitting Linear Mixed-Effects Models using lme4. J Stat Softw 67.

Beermann J, Franke H-D (2012) Differences in resource utilization and behaviour between coexisting Jassa species (Crustacea, Amphipoda). Mar Biol 159:951–957.

Belser LW, Mays EL (1980) Specific Inhibition of Nitrite Oxidation by Chlorate and Its Use in Assessing Nitrification in Soils and Sediments. Appl Environ Microbiol 39:505–510.

Bolyen E, Rideout JR, Dillon MR, Bokulich NA, Abnet CC, Al-Ghalith GA, Alexander H, Alm EJ, Arumugam M, Asnicar F, Bai Y, Bisanz JE, Bittinger K, Brejnrod A, Brislawn CJ, Brown CT, Callahan BJ, Caraballo-Rodríguez AM, Chase J, Cope EK, Da Silva R, Diener C, Dorrestein PC, Douglas GM, Durall DM, Duvallet C, Edwardson CF, Ernst M, Estaki M, Fouquier J, Gauglitz JM, Gibbons SM, Gibson DL, Gonzalez A, Gorlick K, Guo J, Hillmann B, Holmes S, Holste H, Huttenhower C, Huttley GA, Janssen S, Jarmusch AK, Jiang L, Kaehler BD, Kang KB, Keefe CR, Keim P, Kelley ST, Knights D, Koester I, Kosciolek T, Kreps J, Langille MGI, Lee J, Ley R, Liu Y-X, Loftfield E, Lozupone C, Maher M, Marotz C, Martin BD, McDonald D, McIver LJ, Melnik AV, Metcalf JL, Morgan SC, Morton JT, Naimey AT, Navas-Molina JA, Nothias LF, Orchanian SB, Pearson T, Peoples SL, Petras D, Preuss ML, Pruesse E, Rasmussen LB, Rivers A, Robeson MS, Rosenthal P, Segata N, Shaffer M, Shiffer A, Sinha R, Song SJ, Spear JR, Swafford AD, Thompson LR, Torres PJ, Trinh P, Tripathi A, Turnbaugh PJ, Ul-Hasan S, van der Hooft JJJ, Vargas F, Vázquez-Baeza Y, Vogtmann E, von Hippel M, Walters W, Wan Y, Wang M, Warren J, Weber KC, Williamson CHD, Willis AD, Xu ZZ, Zaneveld JR, Zhang Y, Zhu Q, Knight R, Caporaso JG (2019) Reproducible, interactive, scalable and extensible microbiome data science using QIIME 2. Nat Biotechnol 37:852–857.

Boon, A.R., Caires, S., Wijnant, I.L., Verzijlbergh, R., Zijl, F., Schouten, J.J., Muis, S., vanKessel, T., van Duren, L., van Kooten, T., 2018. Assessment of System Effects of Largescale Implementation of Offshore Wind in the Southern North Sea, p. 61 https://doi.org/10.13140/RG.2.2.23113.60000 (Deltares project report number 11202792-002).

Braeckman U, Foshtomi MY, Van Gansbeke D, Meysman F, Soetaert K, Vincx M, Vanaverbeke J (2014) Variable Importance of Macrofaunal Functional Biodiversity for Biogeochemical Cycling in Temperate Coastal Sediments. Ecosystems 17:720–737.

Braeckman U, Provoost P, Gribsholt B, Van Gansbeke D, Middelburg JJ, Soetaert K, Vincx M, Vanaverbeke J (2010) Role of macrofauna functional traits and density in biogeochemical fluxes and bioturbation. Mar Ecol Prog Ser 399:173–186.

Breine NT, De Backer A, Van Colen C, Moens T, Hostens K, Van Hoey G (2018) Structural and functional diversity of soft-bottom macrobenthic communities in the Southern North Sea. Estuar Coast Shelf Sci 214:173–184.

Breteler WCM, Grice K, Schouten S, Kloosterhuis HT and Damsté JSS (2002*). Stable carbon isotope fractionation in the marine copepod Temora longicornis: unexpectedly low $\delta^{13}C$ value of faecal pellets.* Mar. Ec. Progr. Ser. 240: 195-204.

Buck BH, Ebeling MW, Michler-Cieluch T. Mussel cultivation as a co-use in offshore wind farms: potential and economic feasibility. Aquaculture Economics & Management. 2010 Nov 30;14(4):255-81.

Buhr KJ (1976) Suspension-feeding and assimilation efficiency in Lanice conchilega (Polychaeta). Mar Biol 38:373–383.

Buhr K-J, Winter JE (1977) Distribution and maintenance of a lanice conchilega association in the Weser estuary (FRG), with special reference to the suspension)feeding behaviour of Lanice conchilega. Biol Benthic Org:101–113.

Callahan BJ, McMurdie PJ, Holmes SP (2017) Exact sequence variants should replace operational taxonomic units in marker-gene data analysis. ISME J 11:2639–2643.

Callahan BJ, McMurdie PJ, Rosen MJ, Han AW, Johnson AJA, Holmes SP (2016) DADA2: High-resolution sample inference from Illumina amplicon data. Nat Methods 13:581–583.

Caporaso JG, Lauber CL, Walters WA, Berg-Lyons D, Lozupone CA, Turnbaugh PJ, Fierer N, Knight R (2011) Global patterns of 16S rRNA diversity at a depth of millions of sequences per sample. Proc Natl Acad Sci 108:4516–4522.

Causon PD, Gill AB (2018) Linking ecosystem services with epibenthic biodiversity change following installation of offshore wind farms. Environ Sci Policy 89:340–347.

Chen J, Bittinger K, Charlson ES, Hoffmann C, Lewis J, Wu GD, Collman RG, Bushman FD, Li H (2012) Associating microbiome composition with environmental covariates using generalized UniFrac distances. Bioinformatics 28:2106–2113.

Choy SC. Natural diet and feeding habits of the crabs Liocarcinus puber and L. holsatus (Decapoda, Brachyura, Portunidae). Marine Ecology Progress Series. 1986 Jun 19;31(6):87- 99

Clarke KR and Gorley RN (2006). Primer v6: User Manual/Tutorial. Primer-E Plymouth.

Coates DA, Deschutter Y, Vincx M, Vanaverbeke J (2014) Enrichment and shifts in macrobenthic assemblages in an offshore wind farm area in the Belgian part of the North Sea. Mar Environ Res 95:1–12.

Conover RJ (1966) Assimilation of Organic matter by zooplankton. Limnol Oceanogr 11:338–345.

Coolen JWP, van der Weide B, Cuperus J, Blomberg M, Van Moorsel GWNM, Faasse MA, Bos OG, Degraer S, Lindeboom HJ (2020) Benthic biodiversity on old platforms, young wind farms, and rocky reefs. ICES J Mar Sci 77:1250–1265.

Costello C, Cao L, Gelcich S, Cisneros-Mata MÁ, Free CM, Froehlich HE, Golden CD, Ishimura G, Maier J, Macadam-Somer I, Mangin T, Melnychuk MC, Miyahara M, de Moor CL, Naylor R, Nøstbakken L, Ojea E, O'Reilly E, Parma AM, Plantinga AJ, Thilsted SH, Lubchenco J (2020) The future of food from the sea. Nature 588:95–100.

Coughlan J (1969) The estimation of filtering rate from the clearance of suspensions. Mar Biol 2:356–358.

Cranford PJ (2019). Chapter 8: Magnitude and Extent of Water Clarification Services Provided by Bivalve Suspension Feeding. In Goods and Services of Marine Bivalves, pp. 119-141. Ed. By Smaal AC, Ferreira JG, Grant J, Petersen JK and Strand Ø, 598 pp.

De Backer A, Buyse J and Hostens K (2020). *A decade of soft sediment epibenthos and fish monitoring at the Belgian offshore wind farm area*. In *Environmental Impacts of Offshore Wind Farms in the Belgian Part of the North Sea: Empirical Evidence Inspiring Priority Monitoring, Research and Managemen*t. pp. 79-113. Ed. by Degraer S, Brabant R, Rumes B & Vigin L. Royal Belgian Institute of Natural Sciences, OD Natural Environment, Marine Ecology and Management, 133 pp.

De Borger E, Ivanov E, Capet A, Braeckman U, Vanaverbeke J, Grégoire M, Soetaert K (2021) Offshore Windfarm Footprint of Sediment Organic Matter Mineralization Processes. Front Mar Sci 8.

De Luca Peña LV (2016). *Modelling the shadow effect caused by the growth of the blue mussel Mytilus edulis on offshore wind farms in the North Sea*. Master Thesis at Universiteit Antwerpen, Vrije Universiteit Brussel, Universiteit Gent and Royal Netherlands Institute for Sea Research

De Mesel I, Kerckhof F, Norro A, Rumes B, Degraer S (2015) Succession and seasonal dynamics of the epifauna community on offshore wind farm foundations and their role as stepping stones for non-indigenous species. Hydrobiologia 756:37–50.

Degraer S, Carey D, Coolen J, Hutchison Z, Kerckhof F, Rumes B, Vanaverbeke J (2020) Offshore Wind Farm Artificial Reefs Affect Ecosystem Structure and Functioning: A Synthesis. Oceanography 33:48–57.

Degraer S, Wittoeck J, Appeltans W, Cooreman K, Deprez T, Hillewaert H, Hostens K, Mees J, Vanden Berghe E, Vincx M (2006) The macrobenthos atlas of the Belgian part of the North Sea.

Dixon IMT, Moore PG (1997) A comparative study on the tubes and feeding behaviour of eight species of corophioid Amphipoda and their bearing on phylogenetic relationships within the Corophioidea. Philos Trans R Soc Lond B Biol Sci 352:93–112.

Douglas GM, Maffei VJ, Zaneveld J, Yurgel SN, Brown JR, Taylor CM, Huttenhower C, Langille MGI (2019) PICRUSt2: An improved and customizable approach for metagenome inference. Bioinformatics.

Duarte CM, Pitt KA, Lucas CH, Purcell JE, Uye S, Robinson K, Brotz L, Decker MB, Sutherland KR, Malej A, Madin L, Mianzan H, Gili J-M, Fuentes V, Atienza D, Pagés F, Breitburg D, Malek J, Graham WM, Condon RH (2013) Is global ocean sprawl a cause of jellyfish blooms? Front Ecol Environ 11:91–97.

EEA (2022): https://www.eea.europa.eu/ims/european-sea-surface-temperature. Accessed on 10 March 2022

Elliott JM, Davison W (1975) Energy equivalents of oxygen consumption in animal energetics. Oecologia 1975 193 19:195–201.

Fernández-Reiriz MJ, Range P, Álvarez-Salgado XA, Labarta U (2011) Physiological energetics of juvenile clams Ruditapes decussatus in a high CO2 coastal ocean. Mar Ecol Prog Ser 433:97–105.

Forster P, Ramaswamy V, Artaxo P, Berntsen T, Betts R, Fahey DW, Haywood J, Lean J, Lowe DC, Myhre G, Nganga J, Prinn R, Raga G, Schulz M, Van Dorland R (2007) Changes in Atmospheric Constituents and in Radiative Forcing. Chapter 2.

Forster S, Glud RN, Gundersen JK, Huettel M (1999) In situ Study of Bromide Tracer and Oxygen Flux in Coastal Sediments. Estuar Coast Shelf Sci 49:813–827.

Foshtomi MY, Leliaert F, Derycke S, Willems A, Vincx M, Vanaverbeke J (2018) The effect of bio-irrigation by the polychaete Lanice conchilega on active denitrifiers: Distribution, diversity and composition of nosZ gene. PLOS ONE 13:e0192391.

Gadeken K, Clemo WC, Ballentine W, Dykstra SL, Fung M, Hagemeyer A, Dorgan KM, Dzwonkowski B (2021) Transport of biodeposits and benthic footprint around an oyster farm, Damariscotta Estuary, Maine. PeerJ 9:e11862.

Gazeau F, Urbini L, Cox TE, Alliouane S, Gattuso JP (2015) Comparison of the alkalinity and calcium anomaly techniques to estimate rates of net calcification. Mar Ecol Prog Ser 527:1–12.

Gérino M, Stora G, François-Carcaillet F, Gilbert F, Poggiale J-C, Mermillot-Blondin F, Desrosiers G, Vervier P (2003) Macro-invertebrates functional groups in freshwater and marine sediments: a common mechanistic classification. Vie Milieu 53:221–231.

Gnaiger E (1983) Heat dissipation and energetic efficiency in animal anoxibiosis: Economy contra power. J Exp Zool 228:471–490.

Halekoh U, Højsgaard S (2014) A Kenward-Roger Approximation and Parametric Bootstrap Methods for Tests in Linear Mixed Models – The R Package pbkrtest. J Stat Softw 59:1–32.

Heisterkamp IM, Schramm A, Larsen LH, Svenningsen NB, Lavik G, de Beer D, Stief P (2013) Shell biofilm-associated nitrous oxide production in marine molluscs: processes, precursors and relative importance. Environ Microbiol 15:1943–1955.

Hoegh-Guldberg O, R Cai, ES Poloczanska, PG Brewer, S Sundby, K Hilmi, VJ Fabry and S Jung (2014). *The Ocean*. In *Climate Change 2014: Impacts, Adaptation, and Vulnerability. Part B: Regional Aspects. Contribution of Working Group II to the Fifth Assessment Report of the Intergovernmental Panel on Climate Change* [Barros VR, CB Field, DJ Dokken, MD Mastrandrea, KJ Mach, TE Bilir, M Chatterjee, KL Ebi, YO Estrada, RC Genova, B Girma, ES Kissel, AN Levy, S MacCracken, PR Mastrandrea and LL White (eds.)]. Cambridge University Press, Cambridge, United Kingdom and New York, NY, USA, pp. 1655-1731.

Holtmann S, Groenewold A, Schrader K, Asjes J, Craeymeersch J, Duineveld G, Bostelen AJ V., Meer J (1996) Atlas of the zoobenthos of the Dutch continental shelf. Ministry of Transport, Public Works and Water Management, Rijswijk, The Netherlands.

Hutchison Z, Bartley M, Degraer S, English P, Khan A, Livermore J, Rumes B, King J (2020) Offshore Wind Energy and Benthic Habitat Changes: Lessons from Block Island Wind Farm. Oceanography 33:58–69.

Ivanov E, Capet A, De Borger E, Degraer S, Delhez EJM, Soetaert K, Vanaverbeke J, Grégoire M (2021) Offshore Wind Farm Footprint on Organic and Mineral Particle Flux to the Bottom. Front Mar Sci.

Jacobs P, Troost K, Riegman R, van der Meer J (2015) Length- and weight-dependent clearance rates of juvenile mussels (Mytilus edulis) on various planktonic prey items. Helgol Mar Res 69:101–112.

Jak R, Glorius S (2017) Macrobenthos in offshore wind farms : a review of research, results and relevance for future developments. Wageningen Marine Research, Den Helder.

Jakob L, Axenov-Gribanov DV, Gurkov AN, Ginzburg M, Bedulina DS, Timofeyev MA, Luckenbach T, Lucassen M, Sartoris FJ, Pörtner H-O (2016) Lake Baikal amphipods under climate change: thermal constraints and ecological consequences. Ecosphere 7:e01308.

Kellogg ML, Cornwell JC, Owens MS, Paynter KT (2013) Denitrification and nutrient assimilation on a restored oyster reef. Mar Ecol Prog Ser 480:1–19.

Krone R, Dederer G, Kanstinger P, Krämer P, Schneider C, Schmalenbach I (2017) Mobile demersal megafauna at common offshore wind turbine foundations in the German Bight (North Sea) two years after deployment - increased production rate of Cancer pagurus. Mar Environ Res 123:53–61.

Krone R, Gutow L, Brey T, Dannheim J, Schröder A (2013) Mobile demersal megafauna at artificial structures in the German Bight–Likely effects of offshore wind farm development. Estuar Coast Shelf Sci 125:1–9.

Kropko J and Harden JJ (2020). *coxed: Duration-Based Quantities of Interest for the Cox Proportional Hazards Model*. R package version 0.3.3. <https://CRAN.R-project.org/package=coxed>

Kuznetsova A, Brockhoff PB, Christensen RHB (2017) LmerTest Package: Tests in Linear Mixed Effects Models. J Stat Softw 82:1–26.

Langille MGI, Zaneveld J, Caporaso JG, McDonald D, Knights D, Reyes JA, Clemente JC, Burkepile DE, Thurber RLV, Knight R, Beiko RG, Huttenhower C (2013) Predictive functional profiling of microbial communities using 16S rRNA marker gene sequences. Nat Biotechnol 31:814–821.

Leadley P, Proença V, Fernández-Manjarrés J, Pereira HM, Alkemade R, Biggs R, Bruley E, Cheung W, Cooper D, Figueiredo J, Gilman E, Guénette S, Hurtt G, Mbow C, Oberdorff T, Revenga C, Scharlemann JPW, Scholes R, Smith MS, Sumaila UR, Walpole M (2014) Interacting Regional-Scale Regime Shifts for Biodiversity and Ecosystem Services. BioScience 64:665–679.

Okumura Y (2012). *rpsychi: Statistics for psychiatric research*. R package version 0.8. <https://CRAN.R-project.org/package=rpsychi>

Magni P, Montani S, Takada C, Tsutsumi H (2000) Temporal scaling and relevance of bivalve nutrient excretion on a tidal flat of the Seto Inland Sea, Japan. Mar Ecol Prog Ser 198:139–155.

Mavraki N, Degraer S, Moens T, Vanaverbeke J (2020a) Functional differences in trophic structure of offshore wind farm communities: A stable isotope study. Mar Environ Res 157:104868.

Mavraki N, Degraer S, Moens T, Vanaverbeke J (2020b) Functional differences in trophic structure of offshore wind farm communities: A stable isotope study. Mar Environ Res 157:104868.

Mavraki N, Degraer S, Vanaverbeke J (2021) Offshore wind farms and the attraction–production hypothesis: insights from a combination of stomach content and stable isotope analyses. Hydrobiologia 848:1639–1657.

Mavraki N, Degraer S, Vanaverbeke J, Braeckman U (2020c) Organic matter assimilation by hard substrate fauna in an offshore wind farm area: a pulse-chase study. ICES J Mar Sci.

McCartain LD, Townsend M, Thrush SF, Wethey DS, Woodin SA, Volkenborn N, Pilditch CA (2017) The effects of thin mud deposits on the behaviour of a deposit-feeding tellinid bivalve: implications for ecosystem functioning. Mar Freshw Behav Physiol 50:239–255.

McMurdie PJ, Holmes S (2013) Phyloseq: An R Package for Reproducible Interactive Analysis and Graphics of Microbiome Census Data. PLoS ONE 8:e61217.

Mehrbach C, Culberson CH, Hawley JE, Pytkowicx RM (1973) Measurement of the Apparent Dissociation Constants of Carbonic Acid in Seawater at Atmospheric Pressure1. Limnol Oceanogr 18:897–907.

Meire L, Soetaert KER, Meysman FJR (2013) Impact of global change on coastal oxygen dynamics and risk of hypoxia. Biogeosciences 10:2633–2653.

Moulton OM, Altabet MA, Beman JM, Deegan LA, Lloret J, Lyons MK, Nelson JA, Pfister CA (2016) Microbial associations with macrobiota in coastal ecosystems: patterns and implications for nitrogen cycling. Front Ecol Environ 14:200–208.

Nagelkerken I, Munday PL (2016) Animal behaviour shapes the ecological effects of ocean acidification and warming: moving from individual to community-level responses. Glob Change Biol 22:974–989.

Oksanen J, Blanchet FG, Friendly M, Kindt R, Legendre P, McGlinn D, Minchin PR, O'Hara RB, Simpson GL, Solymos P, Stevens MHH, Szoecs E, Wagner H (2019) Vegan: Community Ecology Package.

Pierrot , D.E., Wallace , D.W.R., Lewis , E. (2011) MS Excel Program Developed for CO2 System Calculations.

Pierrot DE, Lewis E, Wallace DWR, Wallace DWR (2006) MS Excel Program Developed for CO₂ System Calculations

Poulin R, Mouritsen KN (2006) Climate change, parasitism and the structure of intertidal ecosystems. J Helminthol 80:183–191.

Quast C, Pruesse E, Yilmaz P, Gerken J, Schweer T, Yarza P, Peplies J, Glöckner FO (2012) The SILVA ribosomal RNA gene database project: improved data processing and web-based tools. Nucleic Acids Res 41:D590–D596.

R Core Team (2019) R: a language and environment for statistical computing. R Foundation for Statistical Computing, Vienna.

Ravishankara, A.R., Daniel, J.S., Portmann, R.W. (2009) Nitrous Oxide (N2O): The Dominant Ozone-Depleting Substance Emitted in the 21st Century. Science 326:123–125.

Reubens JT, Degraer S, Vincx M (2014) The ecology of benthopelagic fishes at offshore wind farms: a synthesis of 4 years of research. Hydrobiologia 727:121–136.

Riisgård HU (2001) On measurement of filtration rates in bivalves — the stony road to reliable data: review and interpretation. Mar Ecol Prog Ser 211:275–291.

Riisgård HU, Egede PP, Barreiro Saavedra I (2011) Feeding Behaviour of the Mussel, Mytilus edulis: New Observations, with a Minireview of Current Knowledge. J Mar Biol 2011:e312459.

Rodríguez-Romero A, Jiménez-Tenorio N, Basallote MD, Orte MR De, Blasco J, Riba I (2014) Predicting the Impacts of CO2 Leakage from Subseabed Storage: Effects of Metal Accumulation and Toxicity on the Model Benthic Organism Ruditapes philippinarum. Environ Sci Technol 48:12292–12301.

van der Schatte Olivier A, Jones L, Vay LL, Christie M, Wilson J, Malham SK (2020) A global review of the ecosystem services provided by bivalve aquaculture. Rev Aquac 12:3–25.

Seaward D (1990) Distribution of the marine molluscs of north west Europe. Council, Nature Conservancy, Peterborough.

Seitzinger S (2000) Scaling up: site-specific measurements to global-scale estimates of denitrification. In: *Estuarine science: a synthetic approach to research and practice.* p 211–240

Shade A, Handelsman J (2012) Beyond the Venn diagram: the hunt for a core microbiome. Environ Microbiol 14:4–12.

Slavik K, Lemmen C, Zhang W, Kerimoglu O, Klingbeil K, Wirtz KW (2019) The large-scale impact of offshore wind farm structures on pelagic primary productivity in the southern North Sea. Hydrobiologia:1–19.

De Smet B, D'Hondt AS, Verhelst P, Fournier J, Godet L, Desroy N, Rabaut M, Vincx M, Vanaverbeke J (2015) Biogenic reefs affect multiple components of intertidal soft-bottom benthic assemblages: The Lanice conchilega case study. Estuar Coast Shelf Sci 152:44–55.

Soares-Ramos EPP, de Oliveira-Assis L, Sarrias-Mena R, Fernández-Ramírez LM (2020) Current status and future trends of offshore wind power in Europe. Energy 202:117787.

Soetaert K, Herman PMJ, Middelburg JJ, Heip C, Smith CL, Tett P, Wild-Allen K (2001) Numerical modelling of the shelf break ecosystem: reproducing benthic and pelagic measurements. Deep Sea Res Part II Top Stud Oceanogr 48:3141–3177.

Soetaert K, Meysman F (2012) Reactive transport in aquatic ecosystems: Rapid model prototyping in the open source software R. Environ Model Softw 32:49–60.

Stief P (2013) Stimulation of microbial nitrogen cycling in aquatic ecosystems by benthic macrofauna: mechanisms and environmental implications. Biogeosciences 10:7829–7846.

Tallec G, Garnier J, Billen G, Gousailles M (2008) Nitrous oxide emissions from denitrifying activated sludge of urban wastewater treatment plants, under anoxia and low oxygenation. Bioresour Technol 99:2200–2209.

Tan K, Zheng H (2020) Ocean acidification and adaptive bivalve farming. Sci Total Environ 701:134794.

Tenore KR and González N (1975). *Food chain patterns in the Ría de Arosa, Spain: an area of intense mussel aquaculture*. In Persoone G. et al. (Ed.) Proceedings of the 10th European Symposium on Marine Biology, Ostend, Belgium, Sept. 17-23 (1975): Population dynamics of marine organisms in relation with nutrient cycling in shallow waters. pp. 601-619

Therneau T (2021). *A Package for Survival Analysis in R*. R package version 3.2-11. URL https://CRAN.R-project.org/package=survival.

Toussaint E, De Borger E, Braeckman U, De Backer A, Soetaert K, Vanaverbeke J (2021) Faunal and environmental drivers of carbon and nitrogen cycling along a permeability gradient in shallow North Sea sediments. Sci Total Environ 767:144994.

Van Hoey G, Birchenough SNR, Hostens K (2014) Estimating the biological value of soft-bottom sediments with sediment profile imaging and grab sampling. J Sea Res 86:1–12.

Van Hoey G, Guilini K, Rabaut M, Vincx M, Degraer S (2008) Ecological implications of the presence of the tube-building polychaete Lanice conchilega on soft-bottom benthic ecosystems. Mar Biol 154:1009–1019.

van Leeuwen S, Tett P, Mills D, van der Molen J (2015) Stratified and nonstratified areas in the North Sea: Long-term variability and biological and policy implications. J Geophys Res Oceans 120:4670–4686.

Voet HEE, Van Colen C, Vanaverbeke J (2022) Climate change effects on the ecophysiology and ecological functioning of an offshore wind farm artificial hard substrate community. Sci Total Environ 810:152194.

Volkenborn N, Polerecky L, Wethey DS, Woodin SA (2010) Oscillatory porewater bioadvection in marine sediments induced by hydraulic activities of Arenicola marina. Limnol Oceanogr 55:1231–1247.

Warren CE, Davis GE (1967) Laboratory studies on the feeding, bioenergetics, and growth of fish. Biol Basis Freshw Fish Prod:175–214.

Watson AJ, Schuster U, Shutler JD, Holding T, Ashton IGC, Landschützer P, Woolf DK, Goddijn-Murphy L (2020) Revised estimates of ocean-atmosphere CO2 flux are consistent with ocean carbon inventory. Nat Commun 11:4422.

Wethey DS, Woodin SA (2005) Infaunal Hydraulics Generate Porewater Pressure Signals. Biol Bull 209:139–145.

Widdicombe S, Beesley A, Berge JA, Dashfield SL, McNeill CL, Needham HR, Øxnevad S (2013) Impact of elevated levels of CO2 on animal mediated ecosystem function: The modification of sediment nutrient fluxes by burrowing urchins. Mar Pollut Bull 73:416–427.

Woodin SA, Wethey DS, Volkenborn N (2010) Infaunal Hydraulic Ecosystem Engineers: Cast of Characters and Impacts. Integr Comp Biol 50:176–187.